Sustainable Energy Technologies and Assessments 46 (2021) 101272

Contents lists available at ScienceDirect

Sustainable Energy Technologies and Assessments

journal homepage: www.elsevier.com/locate/seta

A new internet of things enabled trust distributed demand side management system

Bilal Naji Alhasnawi *, Basil H. Jasim

Department of Electrical Engineering, Basrah University, Basra, Iraq

ARTICLE INFO

Keywords:
Home area network
Photovoltaic
Storage system
Demand side management
Cloud
Microgrid

ABSTRACT

Renewable energy resources (RESs) have come under significant focus to cover the massive demand for electricity. Microgrids are coupled with Demand Side Management (DSM) for saving energy and amplifying energy efficacy. CO_2 discharges, frequency and voltage protocols, RES stochastic nature, Peak to Average Ratio (PAR), and load dynamics are still termed as the most significant challenges for smart microgrids. Novel regulation and management methodologies are required for overpowering them. Internet of Things (IoT) is able to offer adaptive supervision of energy intake and warrant a cost-effective and safe functioning of the smart microgrids. In this study, a new DSM system called Real-Time Electricity Scheduling (RTES) for domestic home energy management is introduced for running the microgrids. The proposed management system seeks to curtail cost payments by optimally programming smart devices and enhancing the consumption of energy. The system comprises two portions: software and hardware. The hardware comprises a Base Station Unit (BSU) and many Terminal Unit (TU). The software comprises the Wi-Fi network programming along with the system protocol. In this paper, Message Queue Telemetry Transportation (MQTT) broker was constructed on TU board and BSU. The proposed technique raises effectual use of energy, thus raising the viability of IoT empowered households in smart cities. The approach impulsively reacts to protective home equipment, power factor correction, and price-centred demand response programmes to contest the key concern of the demand response programs, i.e., constraints in terms of customer's knowledge to react upon obtaining demand response signals. Lastly, a smart microgrids model is experimentally employed to accomplish and corroborate the proposed DSM and control approach. The outcomes of the experiment have substantiated the efficacy and viability of the presented approach and the competence of proposed technique for energy management functioning in various modes. The outcomes endorse the proposed method's ability to obtain an optimum DSM scheme by decreasing the smart microgrids' emission cost, energy cost, and PAR, along with power factor correction.

Introduction

Internet of Things (IoT) refers to a paradigm which connects various digital, real and virtual devices (via information network) to smart environments. It is applicable in many domains like transportation, energy, cities, etc. Internet of Energy is regarded as a revolutionary network of smart grid. It is seen to be a general IoT application in the energy and power sectors. The Energy Internet consists of different techniques and components which are summarised into 3 categories, i.e., (i) power system, (ii) communication system, and (iii) control algorithm. In one study, the researchers stated that the cross-disciplinary nature of Energy Internet has presented several opportunities and challenges, which have to be investigated further and validated [1].

Many studies have reported the use of a microgrid. A microgrid usually consists of Distributed Generator (DGs), loads and system of energy storage. The DGs are generally connected to the microgrids with the help of powered electronic devices and can be regulated using hierarchical controllers for fulfilling different objectives like frequency regulation and active power-sharing [2,3].

Formulation of more effectual energy usage programmes has drawn lot of interest lately. The vital objective is to encourage consumers to enhance their energy use. DSM pertains to cutting-edge technology, such as conceiving, supervising, and executing electrical utility tasks and behaviours. DSM, which conveys a load side control, turns significant in a microgrid. With an enormously amplified demand, frail utilities shed their loads when they cannot meet the energy demand. Nonetheless, because of contingency, the conventional load shedding cannot be

* Corresponding author.
E-mail address: bilalnaji11@yahoo.com (B.N. Alhasnawi).

https://doi.org/10.1016/j.seta.2021.101272
Received 17 October 2020; Received in revised form 2 March 2021; Accepted 19 April 2021

Nomenclature

Abbreviations & Acronyms

RESs	Renewable Energy Resources
DSM	Demand Side Management
PAR	Peak To Average Ratio
IoT	Internet Of Things
BSU	Base Station Unit
TU	Terminal Unit
MQTT	Message Queue Telemetry Transportation
EMS	Energy Management System
DGs	Distributed Generator
DCL	Direct Load Control
LS	Load Shifting
PEV	Pluggable Electric Vehicles
ToU	Time-Of-Use
DRPs	Demand Response Programmes
ESS	Energy-Storage-System
DR	Demand-Response
MAS	Multi Agent System
HEMSaaS	Home Energy Management System as a Service
BI	Business Intelligence
HAN	Home Area Networks
WPDF	Weibull Probability Density Feature
RSA	Responsive Shifting Devices
IP	Internet Protocol
HTTP	Hypertext Transfer Protocol
WSN	Wireless Sensor Network
PF	Power Factor
CT	Current Transformer
PT	Potential Transformer
APFC	Automatic Power Factor Correction
PPI	Primary Peak Current
SPI	Secondary Peak Current
PCTO	Peak Current Transformer Output
PPCTO	Peak To Peak Current Transformer Output
POV	Peak Output Voltage
PIV	Peak Input Voltage
UI	User Interface
MCCU	Main Command And Control-Unit
GUI	Graphical User Interface
RTES	Real-Time Electricity Scheduling
DAES	Day Ahead Electricity Scheduling

performed competently, and there will be loss of supply energy. For higher savings of energy, suppliers attempt to adhere to certain generation patterns. Conversely, customers are urged to decrease their loads utilisation during peak hours or transfer loads to off-peak times [4].

To deal with these complications, storage systems, load curtailment, and DSM are utilised. Curbing of loads moderates the system utilisation aspect. Storage systems are termed as the most costly technology globally. Nonetheless, utilising DSM raises the utilisation aspect, profusely regulates the loads, and decreases costs. DSM is a robust tool that realises diverse load shaping goals. The key task of DSMs is to alter load use quantitatively by conceiving utility or supervising load utilisation tasks [6]. DSM programmes are employed to regulate energy use by consumers on either side. It could oversee the customer load and its native generation. Furthermore, the accessible energy resources are competently managed through DSM methodologies without instating transmission lines or new sources [4]. Peak clipping, direct load control (DLC), load shifting (LS), strategic conservation, strategic load growth, valley filling, and flexible load shape are termed as various DSM methods [5]. Few of the loads can be remotely shut down at a top consumption period to evade system failure by utilising DLC. Based on the time reliance of load, LS is mostly utilised to transfer loads from peak to off-peak periods. The peak clipping technique decreases peak demand, whereas the off peak load demand are engaged by utilising valley filling method. The electricity intake could be considerably enhanced by amalgamating DSM with diverse approaches like electricity tariffs, incentives, and penalties [6].

DSM based on incentive and price are the two key variants. In a price-centred DSM, consumers can regulate their energy intake contingent upon the price of energy (dynamic-tariff). In an incentive-centred DSM, utility cartels few controllable loads contingent upon the levels of generation and/or demand. DSM attempts to even out the power demand curve by urging consumers to use less power during peak times and/or transfer energy use to off peak times. For instance, controllable loads like Heating-Ventilating-and-Air-Conditioning (HVAC) and pluggable electric vehicles (PEV) are sensibly shifted for overpowering the dearth of generation. Such loads could considerably raise the average household load and exacerbate the high Peak to Average Ratio (PAR). Occasionally, rather than evening out the curve, it is advisable to stick to the generation pattern. In either scenario, there is a necessity to regulate use of energy by consumers. Devising an effectual DSM method is fundamentally necessary to engage the diverse kinds of loads efficiently. Reducing the energy sources' emission and operation costs could offer customers higher flexibility. Time-of-Use (ToU) refers to a common pricing tool utilised to realise several demand response programmes (DRPs) such as LS and DLC. Based on gains from price deviations, consumers are urged to oversee their electricity use by utilising ToU tariffs. The prices of various periods are ascertained beforehand; furthermore, consumers can regulate their power bills [4].

To preserve the ecological solidity, sustainability, security, and dependability of microgrids, IoT based technologies are deployed so as to enable dealing with the challenges. IoT is described as a network technology of the future wherein information units like things, people, and processes are linked to internet to produce, gather, share and use information [7]. Of late, IoT technologies have been speedily flourishing as they are fostered and executed for improving microgrid uses. IoT technologies like decentralisation, self-healing, smart metering, and two-way communication are vital means for real-time supervision and regulation of all microgrid variables so as to deploy a supple and smart energy management system (EMS). IoT empowers the microgrid to share info among users, enhance microgrid performance, and improve connectivity of microgrid constituents [8–10]. By gathering and scrutinising RES data through IoT, microgrid management setups would be much more secure. Furthermore, utilities could execute operational tasks like enhancing load balancing, lessening outage investigation periods, detecting the outages, augmenting line voltage, decreasing service costs, and reinstating services sooner. Furthermore, use of IoT know-hows for Energy-Storage-System (ESS), smart households, charging station, EVs, and controllable loads enhance microgrid flexibility and dependability [11]. Additionally, it amplifies energy efficacy by controlling the Demand-Response (DR), gathering information, sharing, and transacting energy. To overpower energy-saving and management issues, an IoT based optimum DSM scheme is fundamentally required. Such scheme has to possess the capability to continuously keep energy in line with prospective trends and evade power peak [12,13].

Related works

In [14] the authors suggested new and more practical theoretical models of the four situations for the peak demand determination. A final number of appliances in the studied field, as expressed by a quasi-

random process for entries or power applications, are presumed to underlie the proposed analysis. In [15] the authors proposed a distributed algorithm for sparse loads in demand management, concentrating on the planning problem of scheduling residential devices. The sparse load change technique eliminates the discomfort of customers. In [16] the authors suggested to the smart grid community a cloud-based multi agent system (MAS) for microgrids. The multi-agent system proposed includes smart household agents and a microgrid agent to reduce the residential microgrid peak load and decrease smart homes' electrical cost. In [17] the authors implemented an island-based microgrid system based on peer-to-peer control architecture. The multi-agent and multi-layer algorithms and design accomplish this peer-to-peer architecture, in which several goals are accomplished. These processes can be run simultaneously by an agent with communication and calculation capabilities which are multi-layer controls. In [18] authors implemented an effective demand-side management system for reducing grid energy consumption's PAR. They analyse consumer habits of energy usage, the price of power, the environment, and other attributes for selecting the best approach to load control in terms of the load curve. They suggest a genetic algorithm for energy storage units and energy-management game theory methods. In [19] Yaghm, et al. proposed a fog/cloud-based system that uses fog (local) nodes and cloud servers (for reliable data storage and high computing power). They have suggested their framework on a Wi-Fi IoT board through the constrained application protocol and use the open-source cloud service ThingSpeak. In [20] the authors present the paradigm of architecture, design, and implementation of IoT-based and cloud-based energy management system that generates a consumer load profile that can be accessed on a remote scope by the company of utilities or consumers. The load profiles of consumers allow utility providers to control and distribute their incentives and encourage consumers to change their energy usage.

A multi-agent system for active network control of distribution networks using DR was developed by the authors in [21]. The goal is to provide the distribution networks operators' transactions to the distribution system operators with a dynamic platform as an applicable and useful tool. In [22] authors introduced a new agent-based system to combine industrial and residential demand's flexibility capacity. In this method, a DR provider is proposed to coordinate the sensitive residential and industrial demand aggregation projects. In [23] authors present a multi-target problem, the solution of which is carried out through an evolutionary algorithm and a working methodology. The multi-target issue is demand response to prices in real-time (RTP). Two goals were taken into account: energy regular and customer satisfaction, both of which were reduced. In [24] the authors suggested an adaptive energy system for island and grid mode. A hybrid system including a distribution grid, photovoltaic systems, and batteries is used for energy supply in the consumer's residential building to meet demand in this reference. The system proposed allows for the coordinated operation of distributed energy resource, where appropriate, to grant essential active power and extra service.

The authors implemented a smart home EMS in [25]. Each home App is linked to an IoT entity, which has a unique IP address, which creates a wide network of wireless devices in this framework. In [26] the authors implemented a new binary backtracking algorithm for controlling energy usage in an ideal timeline control unit for home energy management systems. Binary backtracking algorithm provides an optimum timeline for home appliances, so as to reduce demand for a full load and prepare the operation of domestic appliances at certain periods of the day. A new IoE communication framework for microgrid management has been implemented in [27] authors. The framework is based on a versatile, highly scalable IoT-layered infrastructure integrating DERs (things layer). A new HEM as a Service (HEMaaaS) method, centered on a Q-learning algorithm of the neural network, was proposed by the authors in [28]. In [29], the authors implemented a new energy management system that is used as a fog-based computing service. Flexibility, interoperability, networking, real time and privacy features needed for energy management are provided through the implementation of the fog computing platform. In [30], the authors presented a self-learning system for home management platform based on Multi-Agent System, communications, and interactions between agents were built on the IoT concepts. In [31] the authors implemented and tested a new telemetry-based power factor correction circuit. The key benefit of the equipment was that it can be remotely programmed via the internet connection to make the configuration parameters of the algorithm easy to modify, thus making it possible to work on the basis of the time feedback and artificial intelligence probably better.

For controlling power factor correction switch condensers close to single-phase electrical devices, a microcontroller was used in [32]. The power-factor has different limitations depending on the load. In [33] the authors have provided a method for power-factor correction using optimization-based learning, using cloud to monitor a system in real time, and detect an optimization of the condensers bank algorithm.

To sum up, the introduction of a platform for EMS presents the following noteworthy challenges:

1) Interactivity, output, and interoperability in assorted appliances within an energy management programme.
2) Ability to mould the services, compliance, and scalability of EMS agenda to various types of buildings, houses, and devices.
3) Cost of EMS structure, software and hardware stack employment.

For dealing with the above-stated issues, a new platform for a EMS is proposed, which deploys: scalability, interoperability, flexibility, and connectivity among smart devices based on cloud computing.

The main contributions are mentioned below:

1. We proposed a cost and imported electricity minimisation programme to turn environment greener. Furthermore, we tackle the EMS and sharing economy concern and present an optimum approach to deal with this issue on the basis of cloud computing. The cloud-centred platform is formulated to stow data and share energy between smart consumers.
2. A communication process based on IoT and confirmed stipulations like MQTT, which lets the system to be supple, is proposed in this work. Moreover, Business Intelligence(BI) and analytics are offered in proposed coordination, providing a deep understanding on the data collected by envisaging dashboards and reporting. The use of data storage technologies centred on big data allows system scalability on the national level, rendering energy efficacy systems for domestic owners as well as utility firms.
3. One more contribution of this study is the recommendation of a multi agent system for microgrid representation which assimilates IoT devices for managing energy within buildings. The proposed multi agent system(MAS) is formulated for low-performance hardware like single-board computers. This aids installation of agents in economical and adequately solid hardware in the electrical switchboard of the building. The proposed MAS, nonetheless, uses robust IoT device penetration for delivering energy management solutions inside buildings. This is the most vital contribution by this study.
4. The equipment presented in this study make the most of the progresses in information and communication technology (ICT) to construct a novel telemetry approach and power-factor correction remotely. This technique is multipurpose and supple so as to react to manifold loads, fine-tuning the capacitance phases and power-factor correction unit settings efficiently.

Proposed system description

The demand side management is the key element of smart grid in which customers inform their utilities accordingly of energy usage and the response of the utilities and producers. The cost in real-time is shipped according to customer demand by power utilities. Fig. 1 shows

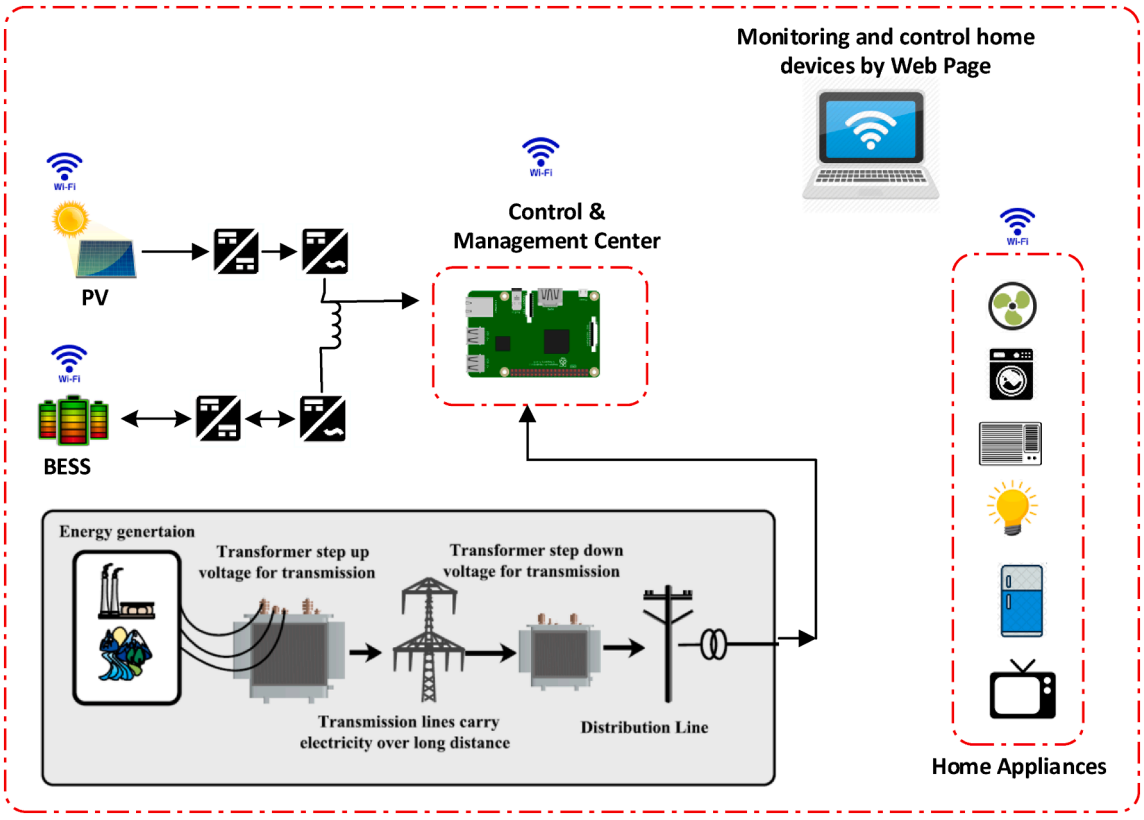

Fig. 1. Proposed microgrid structure.

the proposed demand side management linked to the intelligent grid and the Home Area Networks (HANs). The HAN is linked to the intelligent grid of the DSM subsystems in the intelligent grid. The demand response and energy proficiency are key modules for understanding the importance of smart grid implementation. At its core, IoT is a wide-ranging and comprehensive system of commonplace detailed things linked to internet, adept in identifying themselves and conveying data to the things on the online network. In this paper, IoT is utilised as a web server for Wi-Fi clienteles, signified by Terminal Units (TUs) (Wemos-D1 boards) and utilising the Base Station Unit (RaspberyPi3 boards). All sensors and appliances are linked to the TU. All parameters of home can be connected to internet for formulating IoT structures through such topology. Proposed structure of WeMos-D1 and Raspberry-Pi3 was built for a Message Queue Telemetry Transportation (MQTT) broker. As a gateway for services of IoT, MQTT broker scrutinised and oversaw the smart home gadgets. The benefit of internet portal is that the home appliances can be controlled from any place in the world.

System of photovoltaic power

In microgrid, the output power $\mathscr{W}_{\mathscr{P}\mathscr{V}}$(kW) of photovoltaic is illustrate as [4];

$$\mathscr{W}_{\mathscr{P}\mathscr{V}}(\ell) = \xi_{\mathscr{P}\mathscr{V}} \times \mathscr{A}_{\mathscr{P}\mathscr{V}} \times \mathscr{I}_{r}(\ell)[1 - \mathscr{T}emp_{f}(\mathscr{T}emp_{a}(\ell) - \mathscr{T}emp_{amb})] \quad (1)$$

$$\mathscr{W}_{min} \leq \mathscr{W}_{\mathscr{P}\mathscr{V}} \leq \mathscr{W}_{max} \quad (2)$$

where $\boldsymbol{\xi}_{\mathscr{P}\mathscr{V}}$ is the photovoltaic efficiency (%), $\mathscr{A}_{\mathscr{P}\mathscr{V}}$ is the area of a photovoltaic ($\boldsymbol{m}^2$), $\mathscr{I}_{r}(\ell)$ is the photovoltaic irradiance ($\frac{\boldsymbol{kW}}{\boldsymbol{m}^2}$) at a specific time t, $\mathscr{T}emp_{f}$ is temperatur, $\mathscr{T}emp_{a}$ is the outdoor room temperatures (◦C) and $\mathscr{T}emp_{amb}$ is the ambient room temperatures (◦C).

In order to model a photovoltaic output power hourly distribution and determine its potential, the Weibull probabilty density feature (WPDF) is used. WPDF is given as:

$$f(\mathscr{W}_{\mathscr{P}\mathscr{V}}(\ell)) = \frac{k}{c} \times \left(\frac{\mathscr{I}_{r}(\ell)}{c}\right)^{k-1} \times e^{-\left(\frac{I_r(t)}{c}\right)^{k}} \quad (3)$$

$$\boldsymbol{k} = \left(\frac{\boldsymbol{\eta}}{\overline{\mathscr{A}}}\right)^{-1.086}, and \boldsymbol{c} = \frac{\overline{\mathscr{A}}}{\Gamma(1+\frac{1}{k})} \quad (4)$$

Where Γ is gamma function, $\boldsymbol{\eta}$ is data standard deviation, $\overline{\mathscr{A}}$ is data athematic mean, and. The Levelised photovoltaic cost of energy ($\mathscr{S}_{s}$) ($\frac{\$}{\boldsymbol{kWh}}$) , photovoltaic operating cost ($\mathscr{S}_{\mathscr{P}\mathscr{V}}$) represented as [4];

$$\mathscr{S}_{s} = \frac{\mathscr{S}_{sinv} + \sum_{i=1}^{n} \mathscr{S}_{som}(1+\mathscr{E}_{r})^{-\ell}}{\sum_{\ell=1}^{n} \mathscr{N}_{\mathscr{P}\mathscr{V}\mathscr{A}\mathscr{N}}(1-\boldsymbol{\eta}_{s})^{\ell-1}} \quad (5)$$

$$\mathscr{S}_{\mathscr{P}\mathscr{V}} = \sum_{\ell=1}^{\mathscr{T}} \mathscr{S}_{s} \times \mathscr{W}_{\mathscr{P}\mathscr{V}}(\ell) f(\mathscr{W}_{\mathscr{P}\mathscr{V}}(\ell)) \quad (6)$$

Where $\mathscr{S}_{\mathscr{P}\mathscr{V}}$ is total photovoltaic energy cost, $\mathscr{E}_{r}$ is rate of discount, $\mathscr{S}_{som}$ is photovoltaic operating and maintenance cost, $\mathscr{S}_{sinv}$ is the photovoltaic investment cost ($),$\mathscr{N}_{\mathscr{P}\mathscr{V}\mathscr{A}\mathscr{N}}$ is photovoltaic energy output ($\boldsymbol{kWh}$), $\boldsymbol{\eta}_{s}$ is degradation in photovoltaic, $\boldsymbol{n}$ is photovoltaic lifetime.

Utility grid

Throughout the microgrid peak-demand time, demand is supplied in private from ESS and RES linked to the utility. Conversely, at off- peak times and excess of microgrid generation, energy is diffused to utility as per the utility price. An agreement between utility and microgrid owner is required to let the utility purchase the excess microgrid energy. This would bring down the energy cost of generation unit and decrease a $\boldsymbol{CO2}$ discharge cost. Moreover, the agreement lets the utility to sell energy to the microgrid to meet a demand and enhance dependability. On the basis of the price signal, cost of utility energy $\mathscr{S}_{g}$($) is stated as [4].

$$\mathscr{S}_{g} = \sum_{\ell=1}^{\mathscr{T}} [\mathscr{W}_{gc}(\ell) - \mathscr{W}_{gs}(\ell)]\boldsymbol{\varrho}(\ell) \tag{7}$$

Where $\mathscr{W}_{gs}(\ell)$ is surplus microgrid generation power sold to utility ($\boldsymbol{kW}$), at time t, $\mathscr{W}_{gc}(\ell)$ is microgrid power paid from the utility ($\boldsymbol{kW}$) , $\boldsymbol{\varrho}(\ell)$ is ToU utility price ($\frac{\$}{\boldsymbol{kWh}}$). Cost of utility emission $\mathscr{N}_{g}$($) of expected generator is described as:

$$\mathscr{N}_{g} = \sum_{\ell=1}^{\mathscr{T}} [\boldsymbol{\sigma}\left(\mathscr{W}_{gc}(\ell)\right)^{2} + \boldsymbol{\varsigma}\mathscr{W}_{gc}(\boldsymbol{t}) + \boldsymbol{\tau}] \tag{8}$$

Where, $\boldsymbol{\tau}$ is emission coefficients of utility generators.

Batteries

In this study, batteries is utilised for covering the peak-demand hour shaving and alleviating fluctuations triggered by renewable energy sources. The decisions about discharging and charging battery energy storage system are reliant on price signal obtained from utility. In ToU, if energy price is higher than a stated value, battery energy storage system would discharge, and vice versa. Battery energy storage system would enhance the microgrid's economical functioning, the PAR, and trim the utility's top load. Furthermore, battery is utilised to stow the photovoltaic system excess power generated each time the stowage level is lower compared to upper charge level. Thus, battery energy storage system stowed energy can be stated as below [34].

$$\mathscr{N}_{s}(\ell) = \mathscr{N}_{s}(\ell-1) + \mathscr{H}_{s}\boldsymbol{\xi}_{\mathscr{C}}\mathscr{W}_{ch}(\ell) - \frac{\mathscr{W}_{dch}(\ell)}{\boldsymbol{\xi}_{\mathscr{D}}} \tag{9}$$

where $\mathscr{N}_{s}(\ell)$ is energy stored in battery ($\boldsymbol{kWh}$), $\mathscr{W}_{dch}(\ell)$, $\mathscr{W}_{ch}(\ell)$, are battery discharging and charging power at time t ($\boldsymbol{kW}$), $\boldsymbol{\xi}_{\mathscr{D}}$, $\boldsymbol{\xi}_{\mathscr{C}}$, are discharging and charging efficiency of battery (%), and $\boldsymbol{Ts}$ is time slot duration (hour).

$$0 \le \mathscr{W}_{ch}(\ell) \le \mathscr{W}_{ch}^{max} \tag{10}$$

$$0 \le \mathscr{W}_{dch}(\ell) \le \mathscr{W}_{dch}^{max} \tag{11}$$

$$\mathscr{N}_{s}^{min} \le \mathscr{N}_{s}(\ell) \le \mathscr{N}_{s}^{max} \tag{12}$$

Where $\mathscr{N}_{s}^{max}$ and $\mathscr{N}_{s}^{min}$ are maximum and minimum stored energy in battery ($\boldsymbol{kWh}$), $\mathscr{W}_{dch}^{max}$, $\mathscr{W}_{ch}^{max}$ are maximum battery discharging and charging power ($\boldsymbol{kW}$). The Levelised operational and degradation cost of battery presented as;

$$\mathscr{S}_{\mathscr{B}} = \frac{\left[\mathscr{S}_{\ell inv} + \sum_{\ell=1}^{n}\mathscr{S}_{\ell om}(1+\mathscr{E}_{r})^{-\ell}\right](1+\mathscr{E}_{r})^{-n} - \mathscr{V}_{s}}{(1+\mathscr{E}_{r})^{-n}\mathscr{Z}_{\mathscr{T}f}\mathscr{Z}_{\mathscr{T}c}\mathscr{Z}_{\mathscr{D}c}\mathscr{B}_{\mathscr{R}c}\mathscr{N}_{\mathscr{R}\ell}} \tag{13}$$

where $\mathscr{S}_{\ell inv}$ is the BESS investment cost ($), $\mathscr{V}_{s}$ is battery salvage value, $\mathscr{S}_{\ell om}$ is battery operating and maintenance cost ($), $\mathscr{Z}_{\mathscr{T}c}$ is fading coefficient of normalized capacity, $\mathscr{N}_{\mathscr{R}\ell}$ is BESS rated capacity, $\mathscr{Z}_{\mathscr{T}f}$ is normalised temperature dependent power fading coeficient, $\mathscr{B}_{\mathscr{R}c}$ is battery rated cycle life, $\mathscr{Z}_{\mathscr{D}c}$is depth of discharge (DoD). Therefore, battery operating cost is represented in Eq. (14).

$$\mathscr{S}_{\ell op} = \sum_{\ell=1}^{\mathscr{T}}\mathscr{S}_{\ell}\left(\boldsymbol{\xi}_{c}\mathscr{W}_{ch}(\ell) + \frac{\mathscr{W}_{dch}(\ell)}{\boldsymbol{\xi}_{\mathscr{D}}}\right) \tag{14}$$

Smart device classification

The activities to ensure usability for consumers are being carried out by future users of intelligent devices in homes such as a washing machine, boilers, dishwashing machines, refrigerators, TVs, heating and refreshment units, and lighting devices. There are two main types of appliances below: Shift able appliances are scheduled and controlled over scheduling time via EMS ($\mathscr{T} = 24$).

These devices are designed to reduce the energy charge from one slot to another. Shift able devices have a particular energy load profile, in which adjustable delay occur over guaranteed consumption period. The shiftable device examples are vacuum cleaners, washing machines, dryers, and dishwashers. Suppose the controllable interface set is referred to as $\mathscr{D}_{m,n}$and $\mathscr{d}_{m} = 1, \cdots, \mathscr{D}_{m,n}$ for $n \in \mathscr{N}$ for each user [35].

$$\mathscr{L}_{m,n} = \sum_{\mathscr{d}_{m}\in\mathscr{D}_{m}}\mathscr{L}_{\mathscr{D}_{m,n}} \tag{15}$$

Where $\mathscr{L}_{m,n}$ is manageable appliances loads profiles and $\mathscr{D}_{m,n}$ is manageable appliances sets.

During the operating time $\boldsymbol{t} \in \mathscr{T}$, the energy usage of non-shift able appliances is constant. Non-shiftable devices can't be shifted to off-peak hours for scheduling and reducing the cost. Electrical devices such as energy consumption profiles, including lighting, refrigerators, fans, and TV sets. Let a set of non-shift able devices of user $\boldsymbol{n} \in \boldsymbol{N}$ represented as:

$$\mathscr{L}_{nm,n} = \sum_{\mathscr{d}_{nm}\in\mathscr{D}_{nm}}\mathscr{L}_{\mathscr{D}_{nm,n}} \tag{16}$$

Community-owned electricity is generated from renewable energy sources in the community microgrid (photovoltaic). The optimization model is aimed at planning the limited energy resource for the operation of devices based on their period preference and cost of electrcity. Electrical equipment works under the ToU electricity tariff 24-hour. Where, $\mathscr{L}^{n,\ell}$is users total power consumption of $n \in \mathscr{N}$ in $\ell \in \mathscr{T}$ time slot.

$$\mathscr{L}_{d}^{n} = \mathscr{L}_{m,n} + \mathscr{L}_{nm,n} \tag{17}$$

$$\mathscr{L}_{d}^{n,\ell} = \sum_{\ell=1}^{\mathscr{T}}\mathscr{L}_{d}^{n,\ell} \tag{18}$$

In community of $\mathscr{N}$ users, $\mathscr{L}_{\mathscr{T}}$is total power profile of all users. $\mathscr{L}^{n,\ell}$ denote to power profiles of users $n \in \mathscr{N}$ at $\ell \in \mathscr{T}$,

$$\mathscr{L}_{\mathscr{T}} = \sum_{n\in\mathscr{N}}\sum_{\ell\in\mathscr{T}}\sum_{d\in\mathscr{D}}\mathscr{L}_{d}^{n,\ell}\forall\ell \in \mathscr{T} \tag{19}$$

Each consumer has software for his own energy usage to reduce costs and demand peaks at various times every day. To measure the PAR ratio [35], the aggregated power profil is used. This is form characteristic of all device demand. PAR is defined in Eq. (20),(21), and (22):

$$\mathscr{L}_{peak} = \boldsymbol{max}\mathscr{L}_{\mathscr{T}} \tag{20}$$

$$\mathscr{L}_{avg} = \frac{1}{\mathscr{T}}\sum_{n=1}^{\mathscr{N}}\sum_{\ell=1}^{\mathscr{T}}\mathscr{L}^{n,\ell}\forall\ell \in \mathscr{T} \tag{21}$$

$$\boldsymbol{PAR} = \frac{\mathscr{L}_{peak}}{\mathscr{L}_{avg}} \tag{22}$$

Peak average ratio

The peak to average ratio of the consumer's maximum demand in defined time slot t is represented as the ratio between the average total charge consumed in the indicated time horizon $\boldsymbol{t} = \{1, 2, \cdots, 24\}$. PAR is used for the calculation of the consumption of electricity. The PARs of customers control the functioning of peak services. The PAR of customers should be reduced in order to preserve the supply balance of electricity. PAR can be measured in the following way for M users. [4]:

$$\mathscr{PAR} = \frac{max(\mathscr{N}_{Total}(\ell, m))}{\frac{1}{\mathscr{H}}\sum_{m=1}^{\mathscr{M}}\left(\sum_{\ell=1}^{\mathscr{H}}\mathscr{N}_{Total}(\ell, m)\right)} \tag{23}$$

Energy consumption model

There are three types of microgrid loading equipment. First type related to non-shift able devices like washing machines, cloth-dryers, $= \{\ell_1, \ell_2, \cdots, \ell_u\}$. In this type, users cannot stop devices during their operation until it is completed. Second type is concerned with shift able devices such water pump, vacuum cleaner, $= \{a_1, a_2, \cdots, a_s\}$. In this type,

users can shift their operation to low price time, and when required, their operation can be interrupted after starting. Third type contains fixed devices such refrigerator, air-conditioner, $\mathscr{F} = \{c_1, c_2, \cdots, c_{\mathscr{J}}\}$. In this type, devices operating time can't be modified. these types energy consumpton are given in equations below [36].

$$\mathscr{N}_{a}(\ell) = \sum_{s=1}^{\mathscr{S}} \mathscr{N}_{s}^{a}(\ell)\mathscr{Z}_{s}^{a}(\ell) \tag{24}$$

$$\mathscr{N}_{\ell}(\ell) = \sum_{a=1}^{\mathscr{U}} \mathscr{N}_{a}^{\ell}(\ell)\mathscr{Z}_{a}^{\ell}(\ell) \tag{25}$$

$$\mathscr{N}_{c}(\ell) = \sum_{f=1}^{\mathscr{F}} \mathscr{N}_{f}^{c}(\ell)\mathscr{Z}_{f}^{c}(\ell) \tag{26}$$

Where $\mathscr{N}_{s}^{a}(\ell)$, $\mathscr{N}_{a}^{\ell}(\ell)$ and $\mathscr{N}_{f}^{c}(\ell)$ the energy consumed ($\boldsymbol{kWh}$) by shift able, non-shift able, fixed devices during time t respectively, $\mathscr{Z}_{s}^{a}(\ell)$, $\mathscr{Z}_{a}^{\ell}(\ell)$, and $\mathscr{Z}_{f}^{c}(\ell)$ are the $\boldsymbol{ON/OFF}$ states of shift able, non-shift able, fixed devices, respectively. Energy consumption of total daily can be illustrated as:

$$\mathscr{N}_{\boldsymbol{Total}} = \sum_{\ell=1}^{24} (\mathscr{N}_{a}(\ell) + \mathscr{N}_{\ell}(\ell) + \mathscr{N}_{c}(\ell)) \tag{27}$$

Tariff of time of use (ToU)

The amended ToU tariff is based on additional consumer load demand and generation costs over time. For on-peak and shoulder-peak hour, adjustments per hour are made.

$$\xi_h = \begin{Bmatrix} \mathscr{T}\mathscr{O}\mathscr{U}_h & when \ell_{off} \\ \delta_h & otherwise \end{Bmatrix} \tag{28}$$

Where ξ_h is modified ToU price signal, ℓ_{off} is off-peak hour, h denotes the number of hours. The values of δ depend on extra costs.

The Utilities identify market-specific prices when electricity price is high during high energy demand periods (on-peak hour) and lower durng low power demand period (off-peak hours) [37].

Model of energy pricing

The energy consumption of the appliances is increased by the price signal to determine the energy price. Many electricity charges are available for a one-day lowering of the price of power, such as daily rates (DAP), TOU price, Real Time Price RTP, and peak pricing (CPP). The ToU Prize Program for Users, which limits their consumption at peak hours, is used in this analysis. ToU is called a static price process, as it divides the day into three chunks: off-peak, on peak, mid-peak. The energy costs used daily can be defined as;

$$\mathscr{S}_{\mathscr{T}} = \sum_{\ell=1}^{24} [\mathscr{N}_{a}(\ell) + \mathscr{N}_{\ell}(\ell) + \mathscr{N}_{c}(\ell)]\boldsymbol{\varrho}(\ell) \tag{29}$$

Model of demand response

The microgrid operators may give participants incentives to monitor responsive shifting devices. All responsive shifting devices data, the ratio of total load and the available collection of time slots are recovered and transmitted to microgrid control center. The responsive shifting devices available shifting time slots can be a forward shift, backward shift, or both. Demand response including the reactive power $\mathscr{E}_{\mathscr{R}\mathscr{Q}}$ and active power $\mathscr{E}_{\mathscr{R}\mathscr{P}}$of responsive shifting devices can be illustrate as [4];

$$\mathscr{E}_{\mathscr{R}} = \mathscr{E}_{\mathscr{R}\mathscr{P}} + \boldsymbol{j}\mathscr{E}_{\mathscr{R}\mathscr{Q}} \tag{30}$$

The shifted active/reactive power of responsive shifting devices (RSA) from instant i to t and vice versa (forward $\mathscr{E}_{\mathscr{R}\mathscr{P}f,t}$ and backward $\mathscr{E}_{\mathscr{R}\mathscr{P}b,t}$) can be premeditated using (31) and (32).

$$\mathscr{E}_{\mathscr{R}\mathscr{P}f,t} = \sum_{i,t\in\mathscr{T}} \mathscr{E}_{\mathscr{R}\mathscr{P}i,t} \tag{31}$$

$$\mathscr{E}_{\mathscr{R}\mathscr{P}b,t} = \sum_{i,t\in\mathscr{T}} \mathscr{E}_{\mathscr{R}\mathscr{P}i,t} \tag{32}$$

Whereas time slots number of shift able time $\boldsymbol{\tau}_{\mathscr{M}}$ given in (33).

$$|\boldsymbol{\tau}_{\mathscr{M}}| \leq \ell_f - \ell_s \tag{33}$$

Where (ℓ_f) is the final time and (ℓ_s) is start time. The microgrid

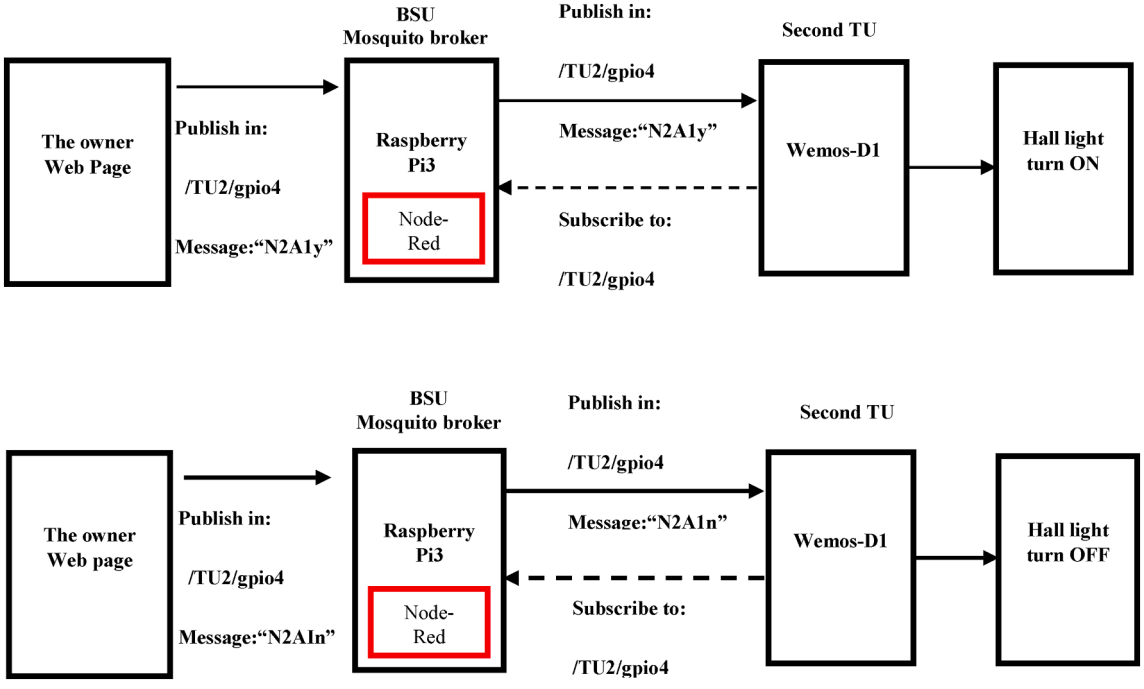

Fig. 2. Examples to follow data between TU and web page via Base Station Unit.

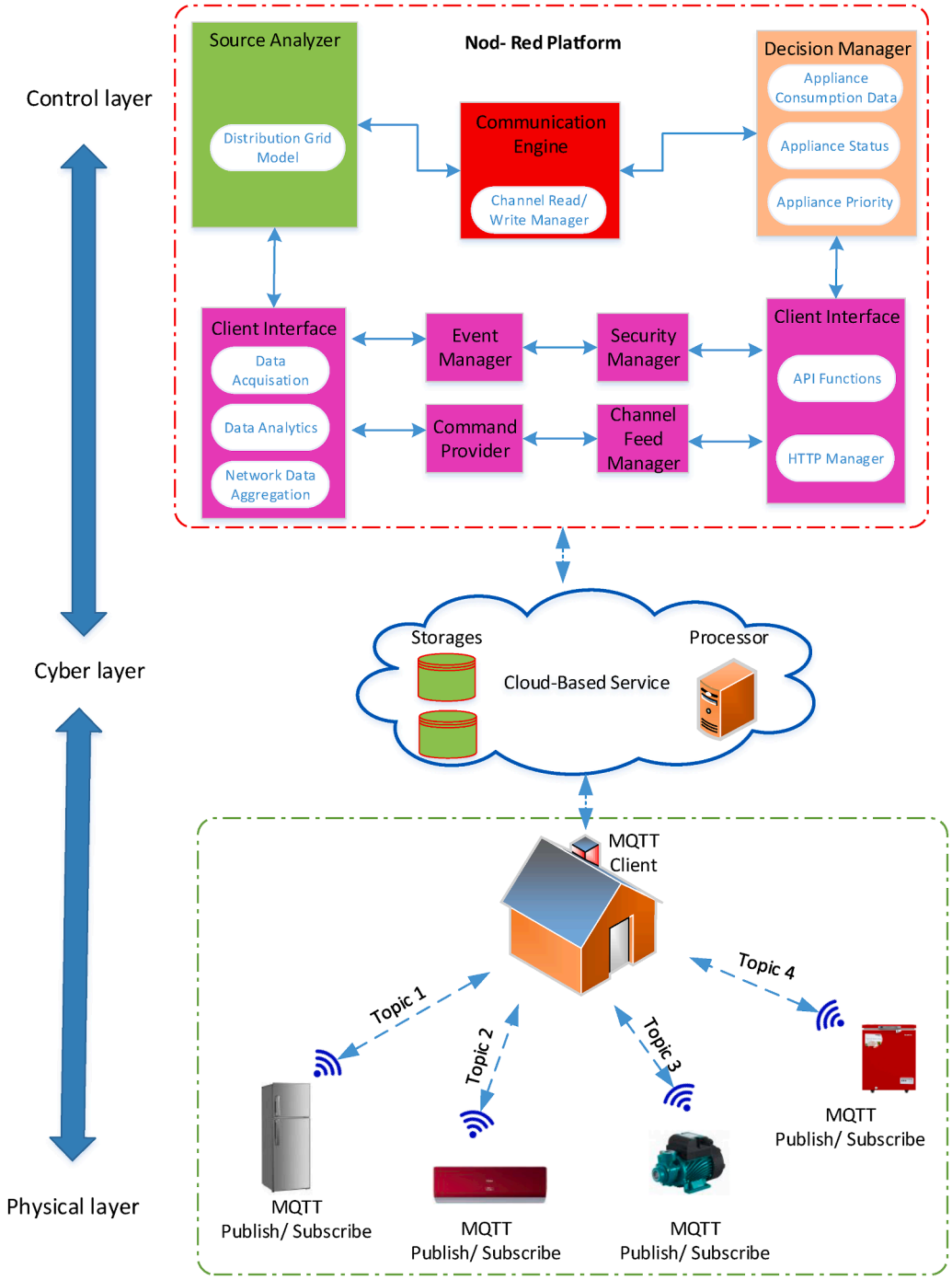

Fig. 3. Smart home proposed architecture of communication.

incentive cost operator can be represented as;

$$\mathscr{S}_t = \sum \mathscr{S}_{dr} \mathscr{E}_{RSP,t} \tag{34}$$

Where $\mathscr{S}_{dr}$ is incentive rate for customers concerning RSA shifting ($/**kW**). Incentive cost rate is defined for off- peak, midpeak, and peak-periods as:

$$\mathscr{S}_{dr} = \begin{cases} \gamma_1 \alpha, t \in \mathscr{H}_1 \\ \gamma_2 \alpha, t \in \mathscr{H}_2 \mathscr{H}_1 \cup \mathscr{H}_2 \cup \mathscr{H}_3 = \mathscr{H} \\ \gamma_3 \alpha, t \in \mathscr{H}_3 \end{cases} \tag{35}$$

where γ_1,γ_2, and γ_3 , values are between 0 and 1, are defined as ToU based scaling factor for the off- peak, midpeak, and peakperiods $\mathscr{H}_1$, $\mathscr{H}_2$, and $\mathscr{H}_3$ respectively.

Problem optimization algorithm

Fig. 11 shows the flow chart of the optimization algorithm. The first level of optimisation is to minimize the cost of operations for photo-voltaic (6), battery energy storage system (14), the cost of energy consumption per day (20), the incentive cost for micro grid and grid emissions as defined in the following equation:

$$minimum \Rightarrow \mathscr{S}_{Total} = \mathscr{S}_g + \mathscr{N}_g + \mathscr{S}_{\mathscr{P}\mathscr{V}} + \mathscr{S}_{our} + \mathscr{S}_{oop} + \mathscr{S}_{\mathscr{T}} \tag{36}$$

The PAR should be minimized as follows to enhance microgrid performance:

$$minimum \Rightarrow \{\mathscr{P}\mathscr{A}\mathscr{R}\} \quad (37)$$

Subject to photovoltaic system (2), and battery energy storage system (9–12), and demand response (33)

Proposed communication platform of energy internet

The home energy-management system have to manage proposed algorithm via integrating historical data coupled with consumer input preference. Therefore, a decision has to be made fast. Moreover, state action pair and user preferences vary speedily during the day and home management over cloud service programme has to provide service in a well-timed manner. In this work, a Linux based fast microcontroller known as RaspberryPi3 has been employed [38]. RaspberryPi3 operates proposed algorithm by using the python programming language. The web-powered Node Red programming model have been chosen for deploying controlling structure of HEMaS platform.

In this study, Base Station Unit and its home gadgets connect through Wi Fi by utilising a lightweight, low power, and safe protocol. MQTT [39] convention is augmented for non-deployable or high latency network. MQTT offers a three-tier network data safeguard. It utilises a broker wherein consumers who subscribe to a specific subject publish message. The subjects are defined inside a home as a sequence of applinces [(Area)/(Appliances)/RaspberryPi3]. Such pattern was utilised by Mosquito [40] broker. The broker backs X.2 certification, username and password safeguard, and client identifier for home energy management system network validation, and therefore meddling can be stopped. For further details, it is assumed that each microcontroler board of TU is recognised via a solitary name, and Fig. 2 shows an examples to follow data between TU and web page via base station unit [36].

Proposed communication architecture

Fig. 3 provides the outline of proposed hierarchy of physical layer, cyber layer and regulating layer smart frameworks. There are two communication layers on proposed hybrid network. In first layer, smart building devices publish MQTT messages to the MQTC Customer Building, and they subscribe to BMC's published MQTT messages for control/protection purposes. The second (globe) layer is an HTTP POST/GET framework for BMC to connect with the cloud. Each device has a Wi Fi module in proposed design, is linked to a local gateway and periodically publishes measures on the subject. Both subjects are subscribed to a cloud channel and are determined by the BMC. The aggregated cloud data can be accessed by node red based cloud interface, which features a built-in device algorithm. The results of the algorithm are transferred from cloud to device through BMC [41].

Hardware of proposed system

Proposed system hardware contains Base Station Unit, an extensive gamut of Terminal Units, freezer, air-conditioner, fans, refrigerator, etc. The details are as follows:

The Base- StationUnit

In proposed system, Base Station Unit(BSU) plays a major role. BSU means coordinator of the overall system. There is a Raspberry Pi3 board in the BSU hardware. The BSU is responsible for testing and disseminating data on the computer to the telephone and web pages of its owner. In order to create wireless connection to which the terminal units will attach, BSU must be established in the Access Point mode. 'Mosquito,' is the open source contact broker running MQTT protocol, is built within BSU. MQTT provide an light weight way to execute messages with the publication/subscription model [36]. Fig. 4 depicts inner construction of Base Station Unit.

Terminal Unit

The terminal units belong to the Wireless Sensor Network (WSN) sub-units. The processor, sensor, wireless communications, and power module are included in each TU.

The TU controller is a Wemos-D1 board responsible for the aggregation, processing, and transmission of sensor data to the BSU [36]. A 5 V DC adapter can be used for each TU. Fig. 5 depicts internal setup of prototype TUs.

Correction of power factor

The power factor is the ratio of real power (kW) to apparent load (KVA) power drawn from electrical load [42]. It can also be defined as using real power to provide total power. Low power generates many problems, including bigger kVA equipment ratings, bigger driver size, low voltage control, increased copper loss, less power handling capacitor etc. Several methods are available for enhancing the system's power factor, such as a synchronous condenser, static trim, static condenser, and so on. [43]. The new approach is more effective and therefore less costly in comparison to other methods and relies on reactive power to

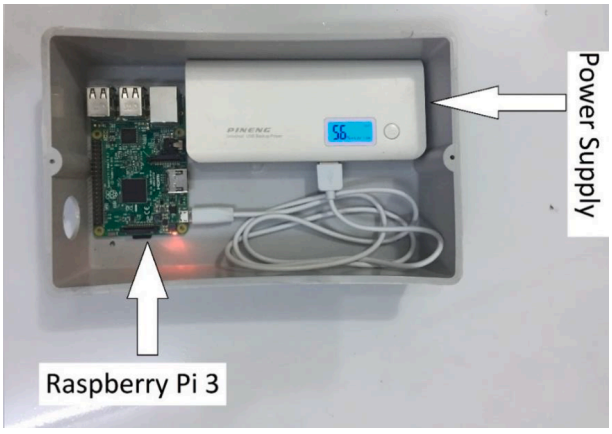

Fig. 4. Internal structure of Base Station Unit.

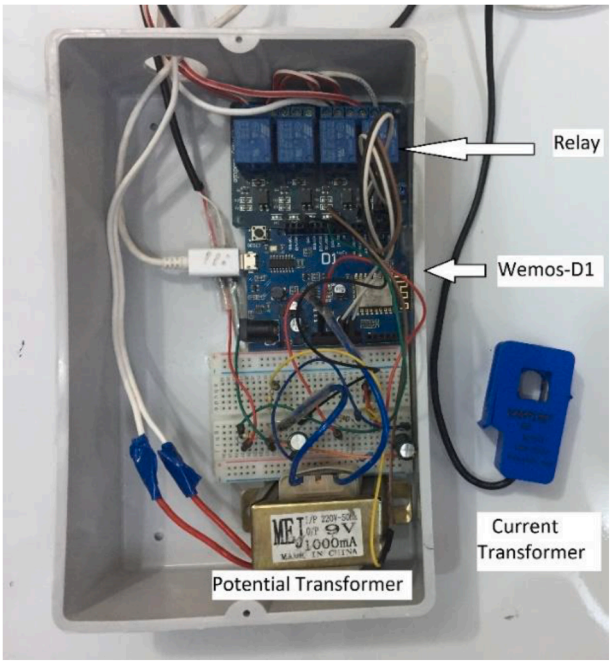

Fig. 5. TUs internal structure.

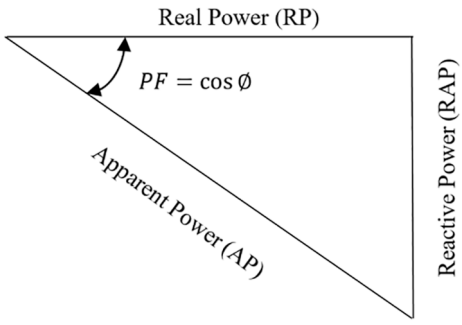

Fig. 6. Power triangle.

overcome these disadvantages. It connects the required capacitance to change PF as closely as possible to uniformity. However, in principle, condensers could deliver 100% of the necessary KVAR, which is virtually united in the correction of PF. As shown in Fig. 6, the power factor can be denoted mathematically.

$$cos\varnothing = \frac{RP}{AP} = PF \tag{38}$$

In the following equations the advantages of improving the power factor can be defined;

$$RP = I \times V \times \cos\varnothing \tag{39}$$

$$I = \frac{P}{V \times \cos\varnothing} \tag{40}$$

$$AP = \frac{RP}{\cos\varnothing} \tag{41}$$

Where *RAP* is Reactive Power, *PF* is Power Factor, *AP* is Apparent Power, *RP* is Real Power, V is Voltage, I is Current.

In non sinusoidal system, Equation change to (41):

$$PF = \frac{RP}{AP} = \frac{RP}{\sqrt{RP^2 + RAP^2 + D^2}} \tag{42}$$

And in cases where reactive power is absent, the power factor remains below 1 since it deforms the non-sinusoidal mechanism directly. Usually, unlike a sinusoidal regime, an annulment of reactive power does not increase power factor. The deformation power is presumably further increased by decreasing reactive power. In other words, power factor may often be worsened in non-sinusoidal mode by incorporating condensers. There is a limit of reactive and deforming variables. The reactive factor is defined as reactive capacity ratio at a single point in the circuit [44,36]:

$$\rho = \frac{RAP}{RP} \tag{43}$$

Where deformation factor is a ratio of deformation power to non deforming power:

$$\tau = \frac{D}{\sqrt{RP^2 + RAP^2}} \tag{44}$$

Equation (42) turns to (43), where $\cos\zeta$ is the notation calculated by (46):

$$PF = \frac{RP}{AP} = \frac{RP}{\sqrt{RP^2 + RAP^2}} \times \frac{\sqrt{RP^2 + RAP^2}}{\sqrt{RP^2 + RAP^2 + D^2}} = \cos\varnothing \times \cos\zeta \tag{45}$$

$$\cos\zeta = \frac{\sqrt{RP^2 + RAP^2}}{\sqrt{RP^2 + RAP^2 + D^2}} < 1 \tag{46}$$

The power factor expression is rewritable as (47):

$$PF = \frac{1}{\sqrt{1+\rho^2}} \times \frac{1}{\sqrt{1+\tau^2}} \tag{47}$$

In a non-sinusoidal device, the power factor is defined not to express how much power is available in the networks as a harmonic source is not network generator but the non– linear receiver.

$$DPF = \cos\varnothing_1 = \frac{RP_1}{AP_1} \tag{48}$$

$$PF = \frac{RP}{AP} = \frac{RP}{I \times V} \tag{49}$$

Depending on current and voltage distortion variables, the expression can be calculated for the total power factor for the non sinusoidal regime. The activepower and apparent power expressions are written to do so. Active power of non sinusoidal system consists in sum of active power which each harmonic in part correspond, producing two components: fundamental, active and harmonic.

$$RP = \sum_{h=1} I_h \times V_h \times \cos(\alpha_h - \beta_h) = \sum_{h=1} I_h \times V_h \times \cos\varnothing_h = P_1 + P_h \tag{50}$$

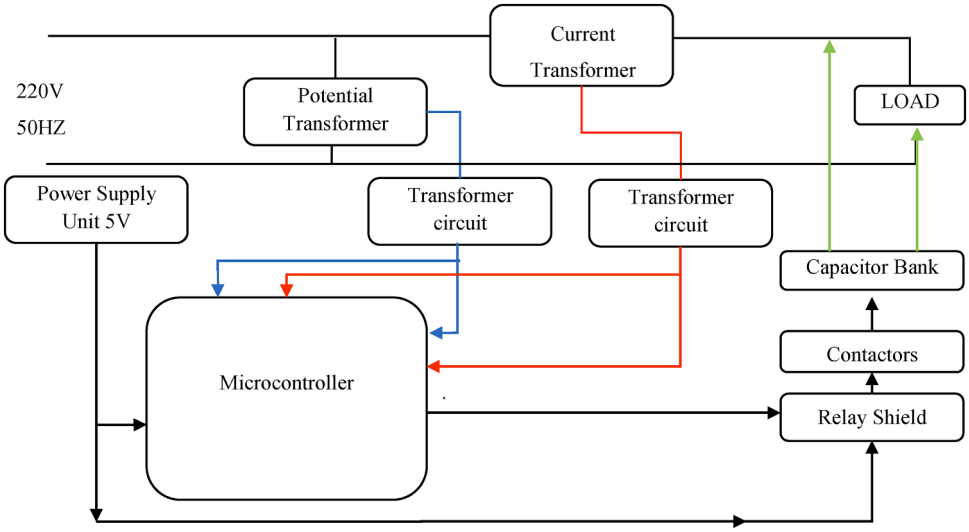

Fig. 7. Proposed APFC diagram.

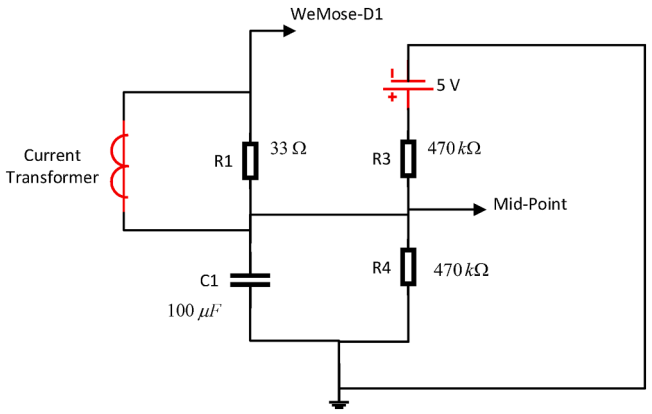

Fig. 8. Diagram of step down current.

$$RP_1 = I_1 \times V_1 \times \cos\varnothing_1 \tag{51}$$

$$RP_h = \sum_{h=1} I_h \times V_h \times \cos\varnothing_h \tag{52}$$

A microcontroller device was used to monitor the process for inserting condensers in the proposed APFC (Automated Power Factor Recreation). Three condensers, connected in series with the condensers and the microcontroller, were used for construction of the APFC. The system's microcontroller role is to read current, voltage, and power factor of the system. The number of condensers should be added to increase power factor to compute microcontroller then. Microcontrollers, interface circuits (PF, stress, current), condensers, relays, contactors are the key components of the APFC device.

Our system supplies up to 220 V and transmits the signal that can be transmitted to the microcontroller by a possible transformer (PT), and transforms this 9 V AI into less than 5 V [36]. In order to calculate the current, CT (Current Transformer) is linked to load. The current transformer output is supplied to current sensing circuit. This circuit output is connected to module's analog input. The PF calculation module of the microcontroller controls the switchover of the condensers. The proposed APFC scheme was illustrate in Fig. 7.

Measurements of current

The current Current Transformer output needs to be scaled and signal matches voltage range of analog input channel of the microcontroller to link the Current Transformer to the microcontroller. The existing diagram of sensor system is demonstrated in Fig. 8.

The current transformer signal is needed to generate a signal that crosses the resister for resistance calculation. Since current limit is 100 A, same value as current transformer current is chosen. The current peak value is set as [36]:

$$PPI = \sqrt{2} \times I = 1.41 \times 100 = 141A \tag{53}$$

Where I is RMS Current and, *PPI* is Primary Peak Current, In addition, the secondary spindle current is indicated by:

$$SPI = \frac{PPI}{N} = \frac{141}{2000} = 70mA \tag{54}$$

Where N is turns Number and *SPI* is Secondary Peak Current.

The load resistor should be equal to half the reference voltages of the microcontroller when running under a peak current to improve the voltage resolution.

$$BurdenResistance(BR) = \frac{\frac{RMV}{2}}{SPI} \tag{55}$$

$$= 2.5V/0.0707A = 35.36\Omega$$

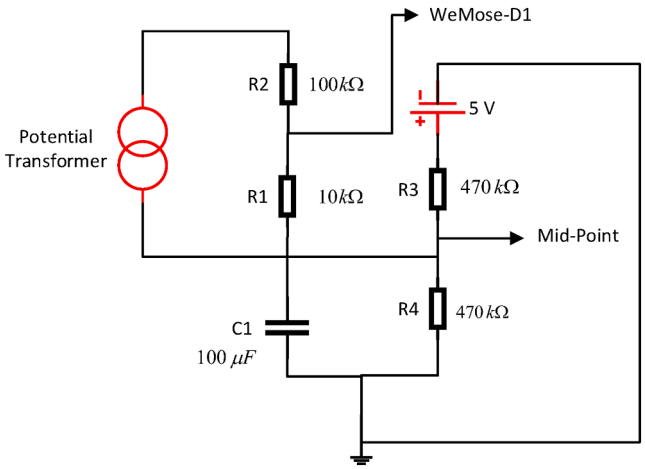

Fig. 9. Circuit diagram of step down voltage.

$$PCTO = \sqrt{2} \times I = \sqrt{2} \times 50mA = 70.71mA \tag{56}$$

Where *PCTO* is PeakCurrent TransformerOutput

$$PPCTO = 2 \times PCTO = 2 \times 70.71mA = 141.42mA \tag{57}$$

Where *PPCTO* is Peakto PeakCurrent TransformerOutput

$$PPV = PPCTO \times BR \tag{58}$$

$$= 141.42mA \times 33\Omega = 4.66V$$

$$Positivepeak = \frac{5}{2} + \frac{4.66}{2} = 4.83V$$

The negative peak is determined with Eq. (88) as:

$$Negativepeak = \frac{5}{2} - \frac{4.66}{2} = 0.16V$$

Measurements of voltage

The transformer potential (PT) converts 220 V to 9 V in the proposed device as shown in Fig. 9. The 9 V device voltage has to be reduced to the level compatible with the Analog Input Microcontroller range to read the main power voltage (0 to 5 V).Fig. 10.

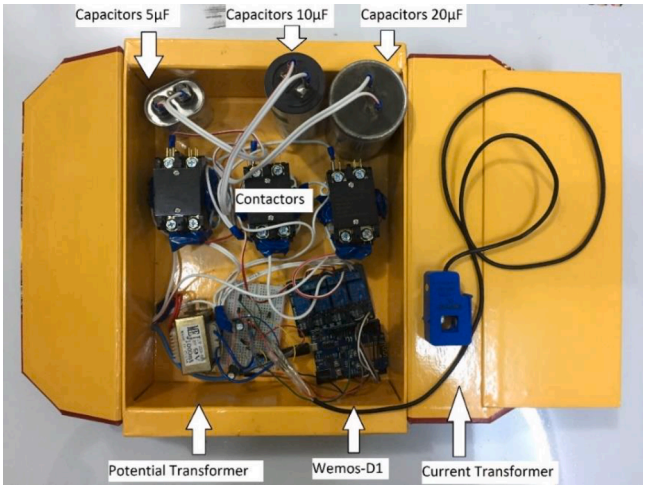

Fig. 10. Complete APFC system.

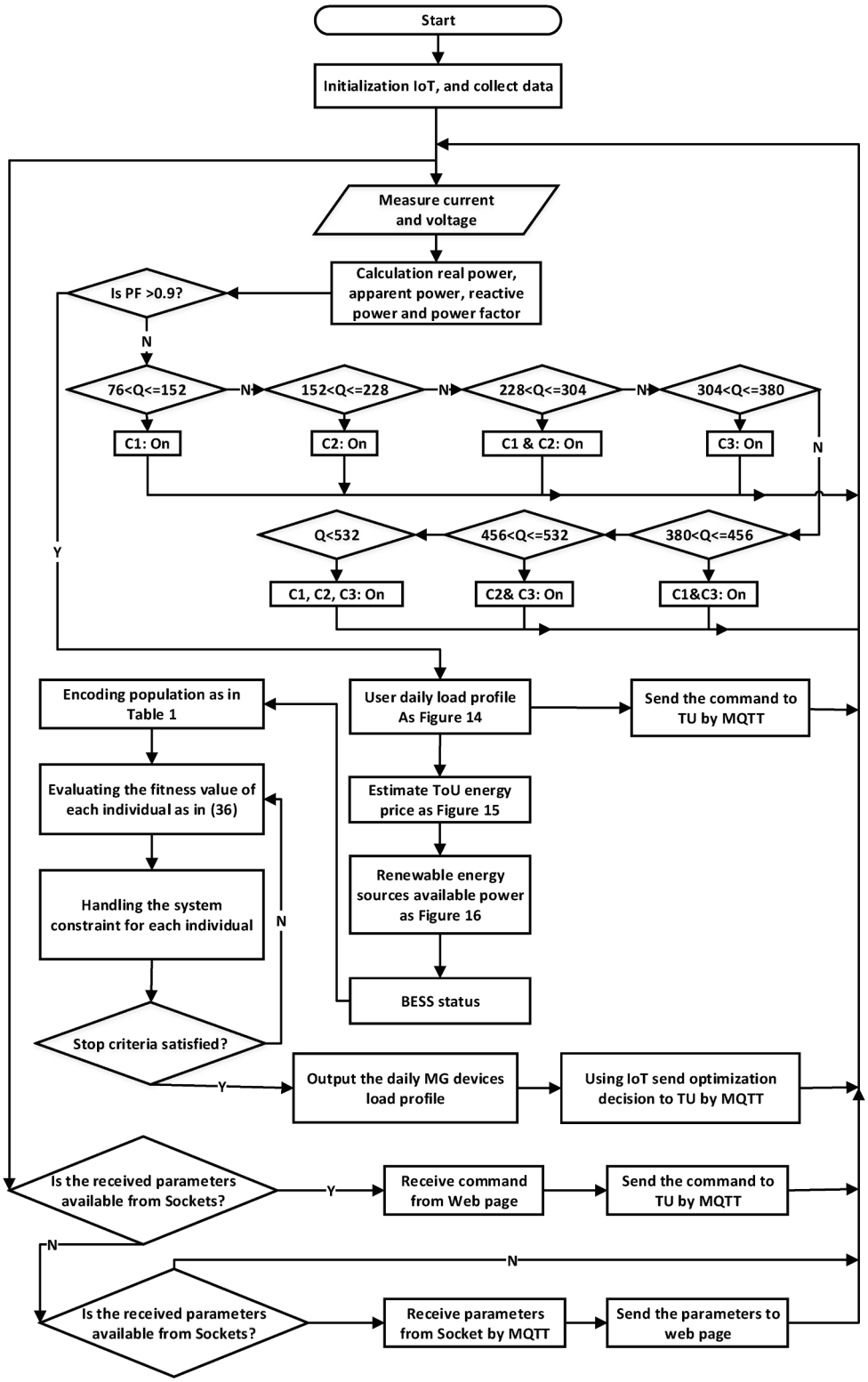

(a)

Fig. 11. Flowchart of proposed system, (a) flowchart of base station unit, (b) flowchart of terminal units.

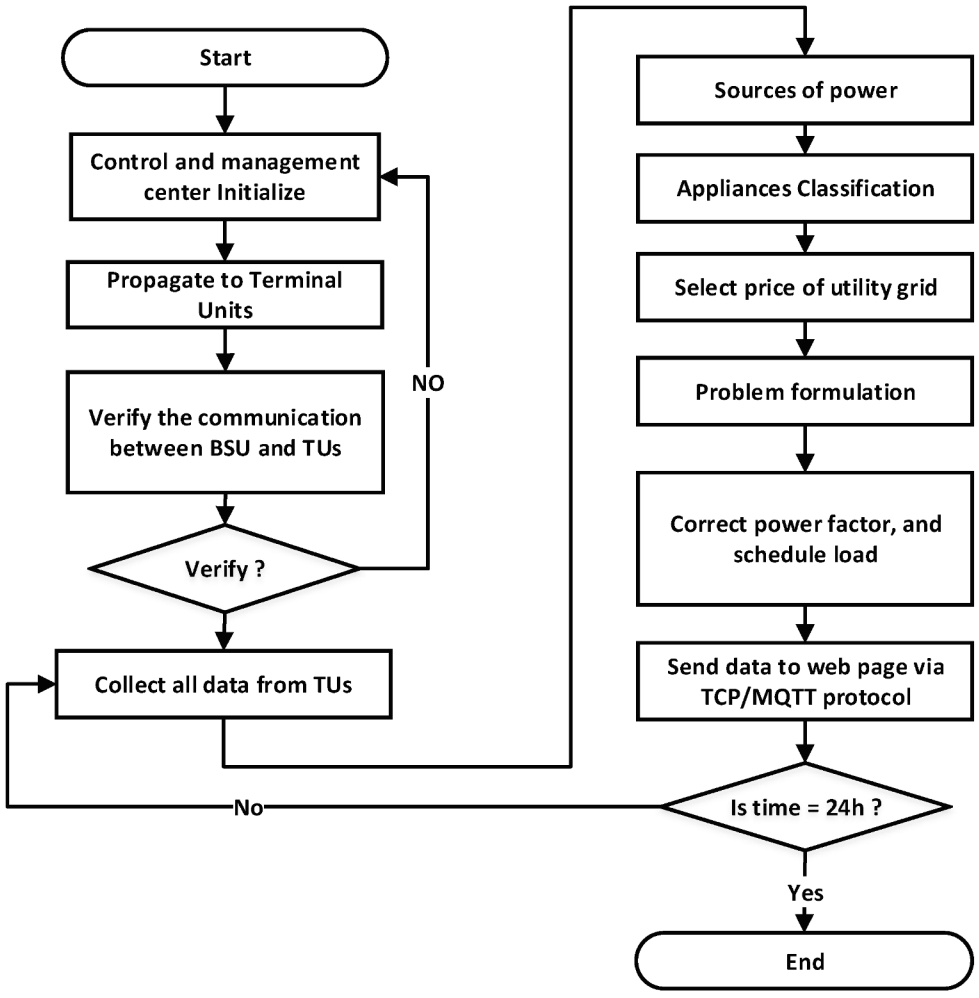

(b)

Fig. 11. (*continued*).

To determine power factor, actual power and apparent power, an RMS voltage measurement is required. The transformer potential scale down, separate from the main high voltage, can be used to calculate the path through the AC to AC transformer potential. To change the signal obtained from the transformer potential output, a signal conditioning circuit is used. A 9 V AC positive limit is + 12.727 V; negative maximum is −12.727 V. The transformer output needs to be converted to signal from 0 V to 5 V, i.e. positive peak < 5 V and the negative limit greater than 0v [36].

Transformer potential output of the sinusoidal waveform is reduced by connecting the transformer terminals via voltage splitting devices. The signal level change is accomplished by adding another power divider output that is attached to the power supply of the microcontroller. In other words, a positive voltage range between 0 V and analog and digital converter (ADC) reference voltage is used to satisfy the requirements of microcontroller analog input signals (5 V). The voltage sensing circuit scheme is illustrate in Fig. 9.

$$POV = \frac{R1}{(R2+R1)} \times PIV = \frac{10k}{(10k+100k)} \times 12.72 = 1.156V \quad (59)$$

Where *PIV* is Peak Input Voltage, and *POV* is Peak Output Voltage

$$PPV = 2 \times POV = 2 \times 1.156 = 2.312V \quad (60)$$

Where PPV is Peak to Peak Voltage.

Resistors R3 and R4 have 470 k ohm resistances and allowed the signal transmission of the voltage [36]. The other microcontroller also uses 5 V, and the resulting waveform is sinusoidal.

$$Positivepeak = \frac{RMV}{2} + \frac{PPV}{2} = \frac{5}{2} + \frac{2.312}{2} = 3.656V \quad (61)$$

Where RMV is the Reference Microcontroller Voltage :

Table 1
Microgrid devices characteristics [4].

Type	Daily usage	Power (kW)	Devices
Devices of Fixed loads	24	0.25	Refregrator
	5	3	HVAC
	8	0.2	TV
	9	0.25	Lights
	18	0.3	PC
	24	0.1	Cameras
	3	1	Oven
Devices of Non shiftable loads	3	1.5	Washing machine
	4	1	Clothes Dryer
	2	1	Dishwasher
	2	1.2	Electric frying pot
Devices of Shiftable loads	6	1.5	Water heater
	3	1.7	Vacuum cleaner
	4	1	Water pump
	2	3.5	gayser

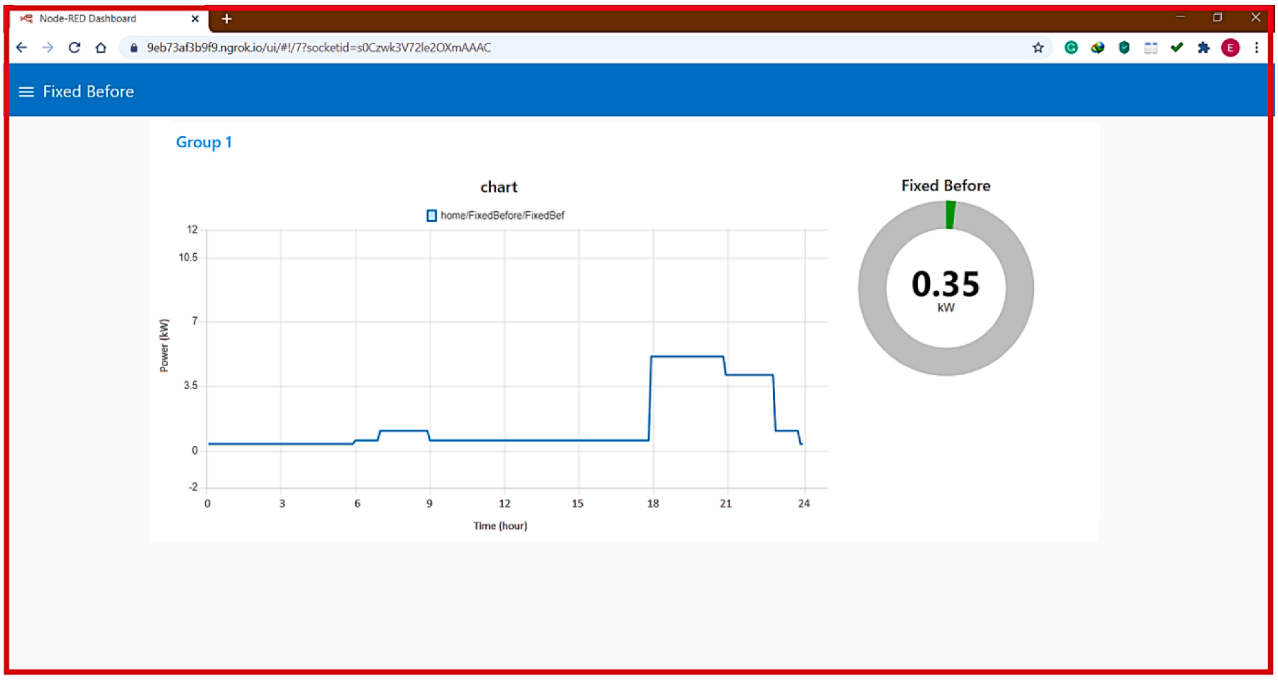

(a)

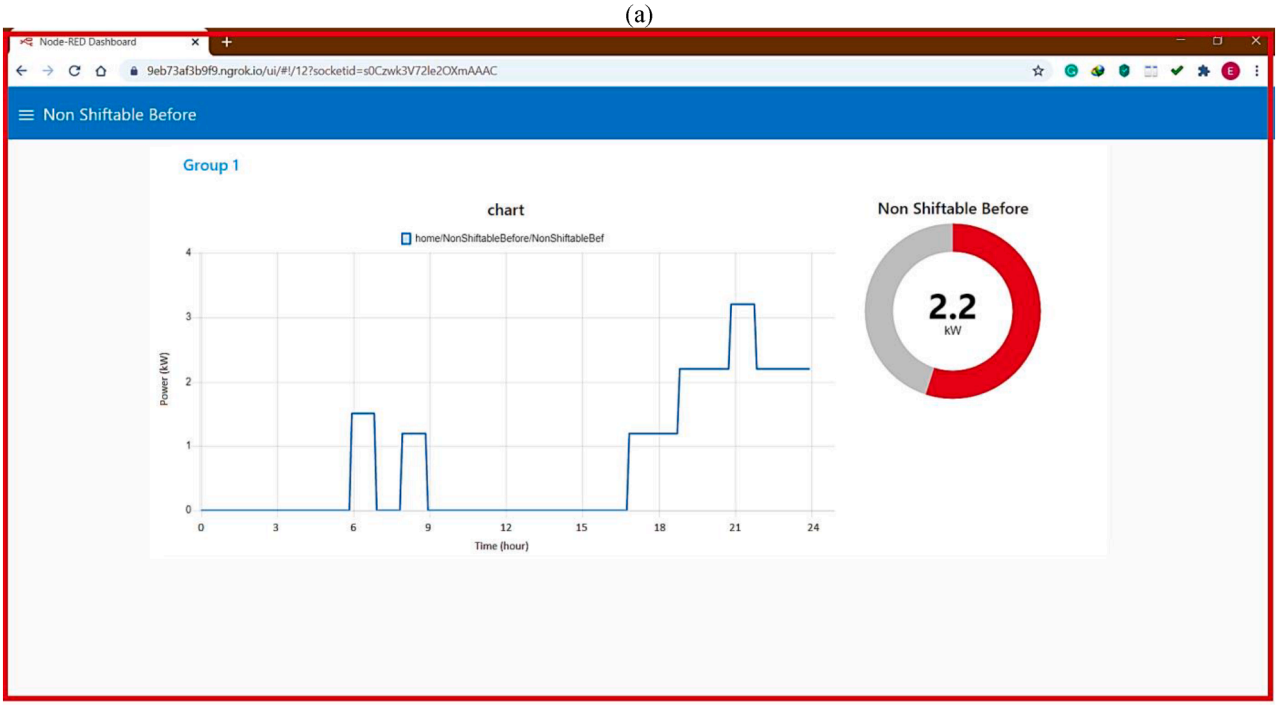

(b)

Fig. 12. Graphical user interface of daily microgrid without proposed energy management system, (a) fixed load, (b) non shift able loads, (c) shift able loads.

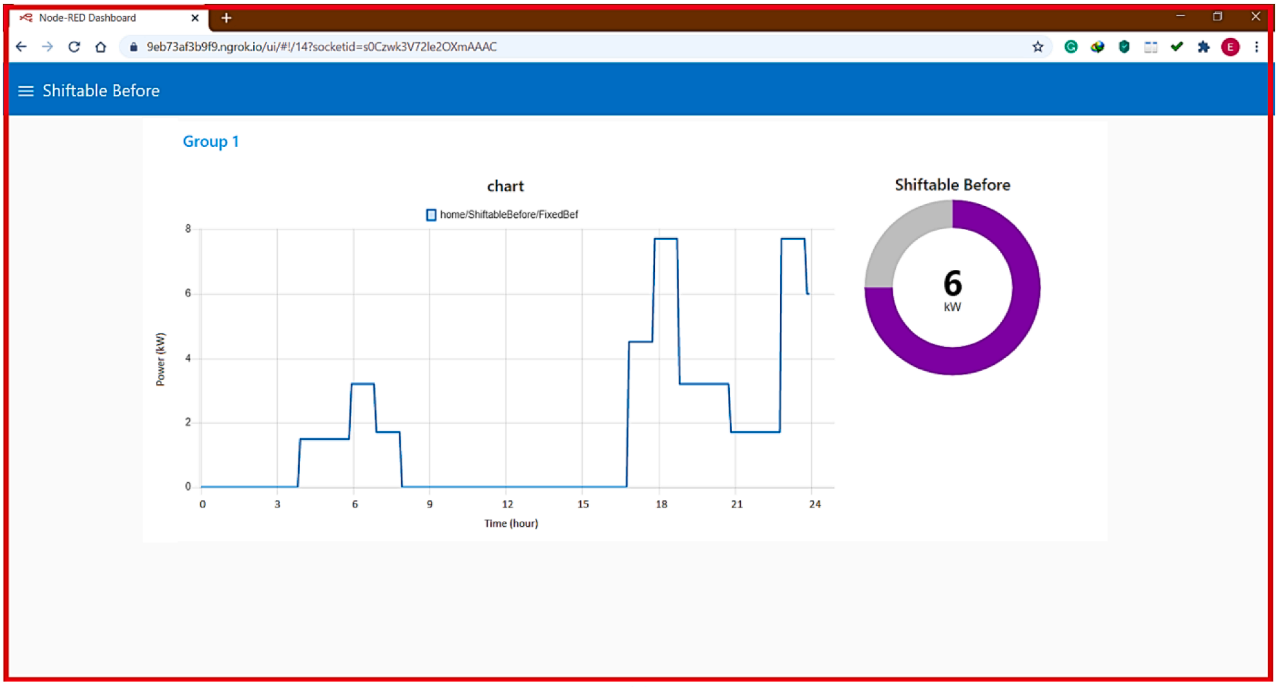

(c)

Fig. 12. (*continued*).

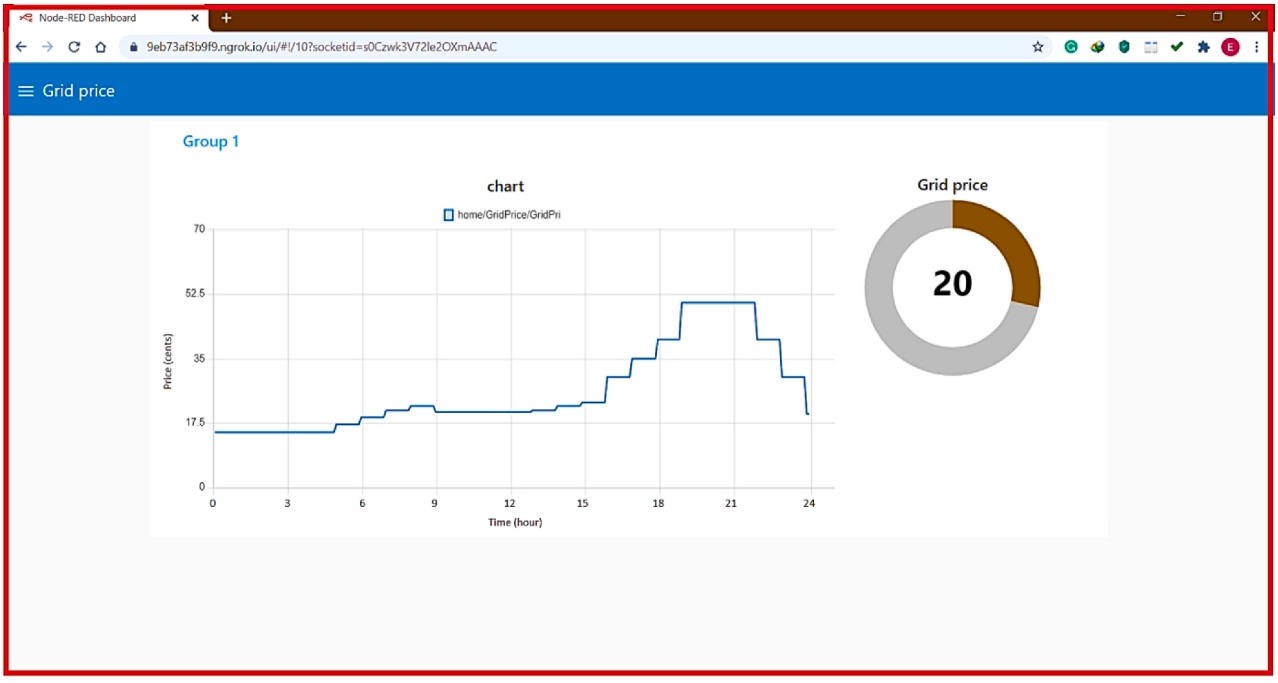

Fig. 13. GUI of Daily utility price signals.

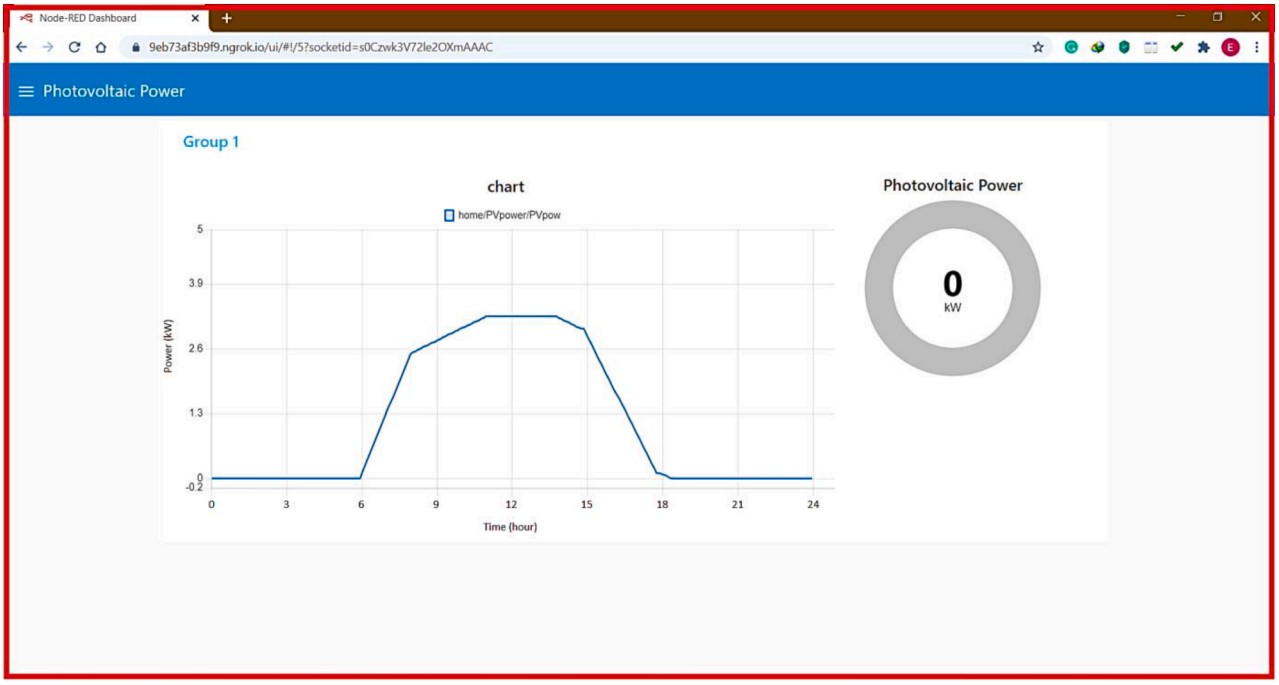

Fig. 14. GUI of daily photovoltaic output power.

$$Negativepeak = \frac{RMV}{2} - \frac{PPV}{2} = \frac{5}{2} - \frac{2.312}{2} = 1.344V \tag{62}$$

The capacitor banks

The condenser banks have different condensers in their collection. The shunt relation of different condensers provides the capability domain required to compensate for a low power factor. The condenser size of the condensers are determined by the electric charge according to the required reactive capacity. In proposed method capacitors is selected as 5μF, 10μF and 20μF.

$$RAP = \sqrt{(AP)^2 - (RP)^2} \tag{63}$$

Fig. 15. GUI of loads power factor before implement suggested power factor correction algorithm.

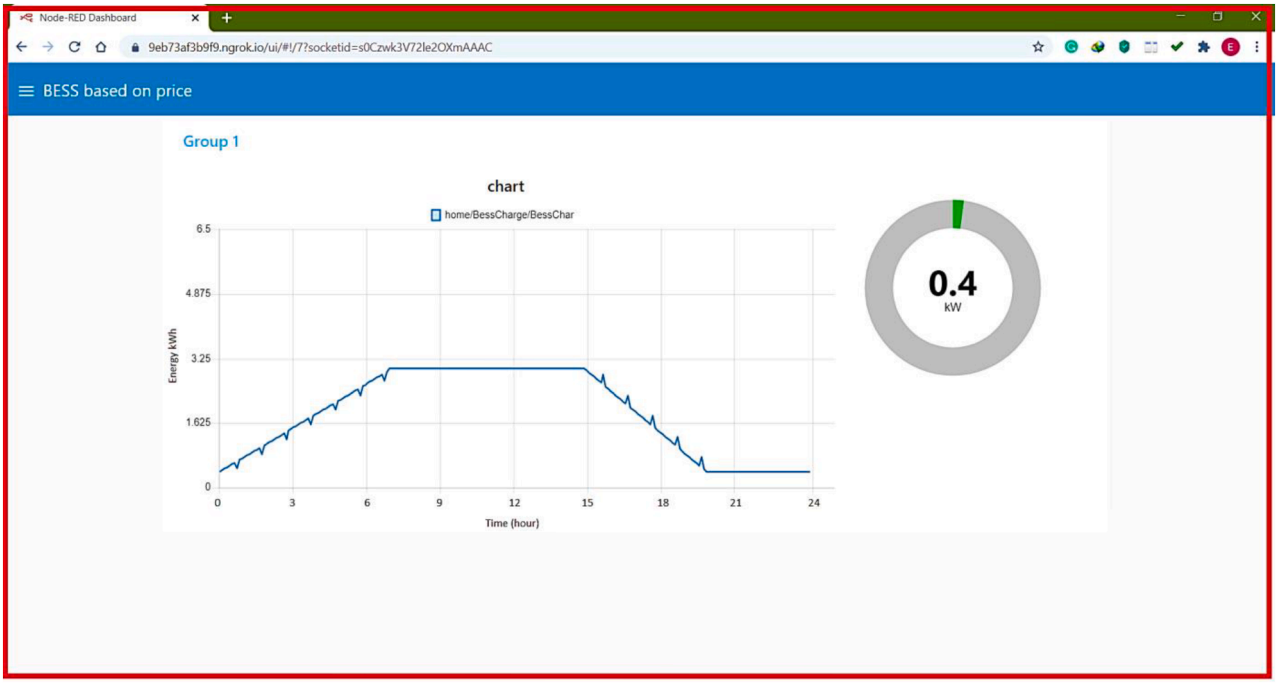

Fig. 16. Graphical user interface of battery based on prices.

$$C = (RP/2\pi fV^2) \tag{64}$$

$$RAP = V^2 \times 2\pi fC \tag{65}$$

Where C is the Capacitance in Farad

$$Reactivepowerof\,20\mu F = 5 \times 10^{-6} \times 50 \times 2 \times 20 \times 3.14 \times 220^2 = 304VAR$$

$$Reactivepowerof\,10\mu F = 5 \times 10^{-6} \times 50 \times 2 \times 10 \times 3.14 \times 220^2 = 152VAR$$

$$Reactivepowerof\,5\mu F = 5 \times 10^{-6} \times 50 \times 2 \times 5 \times 3.14 \times 220^2 = 76VAR$$

Experimental results

This segment outlines the outcomes of Energy Management as a Service over Cloud platform with proposed algorithm to regulate appliances in a sample household. As elucidated in the communication interface and software architecture, the MainCommand and Control-Unit(MCCU) comprises a Raspberry-Pi3 employing a node- red platform. MQTT(Mosquitto) is utilised as broker among subscribing home gadgets and MCCU publisher. A custom python code with proposed algorithm set up on it functions on RaspberyPi3 to regulate home devices across an MQTT gateway. The Node- Red dashboard interface devised in this study provides a simple and suitable user interfac (UI) for a home-owner for interacting with HEMS setup.

The best optimal schedule for home appliances and consumer loads can be difficult to achieve to minimize electrical power consumption costs during demand response (DR) events using simple rules. It is also difficult. For planning of home appliances, some advanced optimisation techniques are therefore needed. Three sub-components are included in the ideal schedule controller, which include client schedule conditions, optimisation technologies, and the architecture of proposed schedule controller. The customer's comfort preferences and device's priority are compared by air condition temperature and water level of the tank on several sets, including load priority, power usage and the customer's preference.

Proposed system protocol

The base station unit receives a command from a web page when the program starts service and sends the command with an address to a Terminal Units. Per TU receives BSU addresses. If TU address matches the address received from BSU, a message is mixed together and the commands that are in that message are applied. Each TU transmits the indicated factors in the message and sends them with the address to the BSU. This data is transmitted by the BSU to the website to collect sensed data from every TU. Fig. 11 displays the flow diagram of the suggested BSU website structure (a). Fig. 11 demonstrates the TU flowchart (b).

Internet WebPage Access

Internet Protocol (IP) is the local port for Raspberry Pi3 IP 1880 dedicated to a web page, which has been used for accessing the local webpage. The IP is http://192.168.0.104:1880/ui local.Ngrok is used to broadcast the web page over the internet. Ngrok helps to convert the local IP address to a global IP address, so that the page can be accessed from any location in world through internet. The web page http://9eb73af3b9f9.ngrok.io is accessible during Ngrok server for web page. Table 1 illustrates microgrid devices characteristics.

Results without correctve method

The home management system includes Graphcal User Interface (GUI) and associated software to assist customers in monitoring total

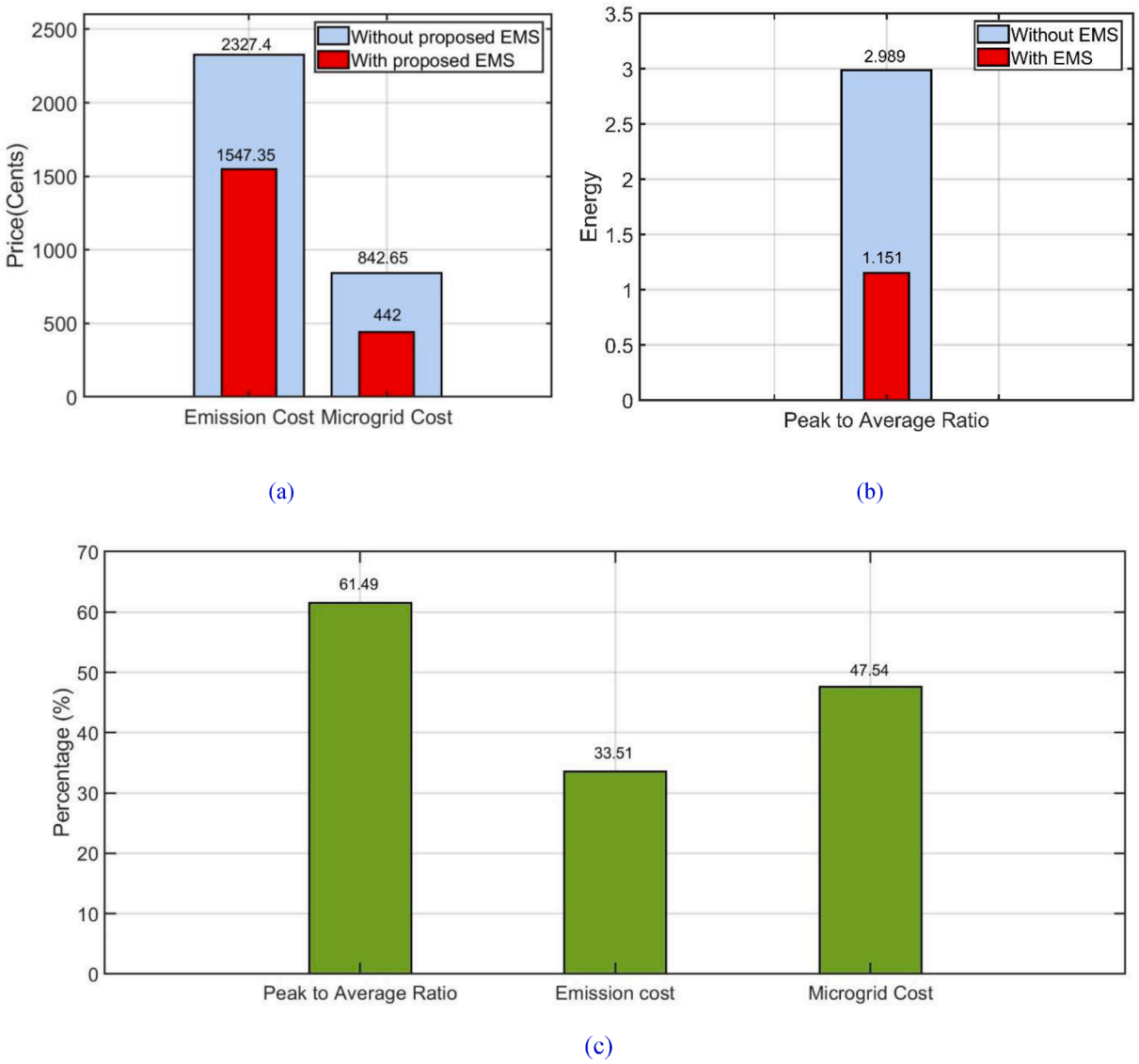

Fig. 17. Comparison between without proposed EMS and with proposed EMS, (a) Emission cost, microgrid cost, (b) peak to average ratio (c) improvement (%).

and individual power consumption, cost, monitor voltage of home devices, monitor current of home appliances, monitor apparent power of home appliances, monitor power factor of home appliances, before implement the proposed algorithm as shown in Fig. 15.

The power consumption data in real time is collected for 24 h at weekday in Iraq. Time slots and demand for every load group are shown in Fig. 12. This figure depicts all customers' daily microgrid demand with three kinds of devices, and its operation time periods are signified. This curve has been attained from every consumed day-to-day energy plan by utilising IoT and microgrid data stowage from consumers' habits and routines. Actual price signal of utility consumed energy is depicted in Fig. 13. Estimated photovoltaic is depicted in Fig. 14.

In this work, batteries discharging and charging procedure relies mainly on actual utility price signals, historical energy price data, and requisite battery discharging and charging period. Microgrid operator ascertains a starting price at which battery begins to charge and discharge. Moreover, battery price is restricted at 25 cents. Thus, to maximise the gains and obtain an effectual performance, battery is charged after utility pricing signal is below 25cents and is discharged when the utility pricing signal is more than 25 cent. Fig. 16 depicts everyday battery performance. The discharging and charging procedure is centred on the utility price signal defined in Fig. 13. After the price signal is below 25 cent, the system has acquired its demand mostly from the utility as the utility price is low. Nevertheless, if price of utility signal is more than 25 cent, consumers are supplied from battery and renewable energy sources.

Results with correctve method

Actual data reflecting a residential sector in Iraq were used to show efficacy of proposed algorithm. Those figures include total watts usage in peak hours from 00:00 until 12:00 PM hours in residential buildings.

With implementing proposed energy management system, it is notable that microgrid consumed energy cost have been decreased from 842.65cents to 442 cents (47.54% of the operation cost), as depicted in Fig. 17. A comparison of energy used up from utility with and without proposed energy management system is made in Fig. 17. Peak-to-average ratio has been decreased. Furthermore, a substantial decrease in the power from the utility and load's peak value has been noted. For same load, the utility's energy intake has not been altered with and

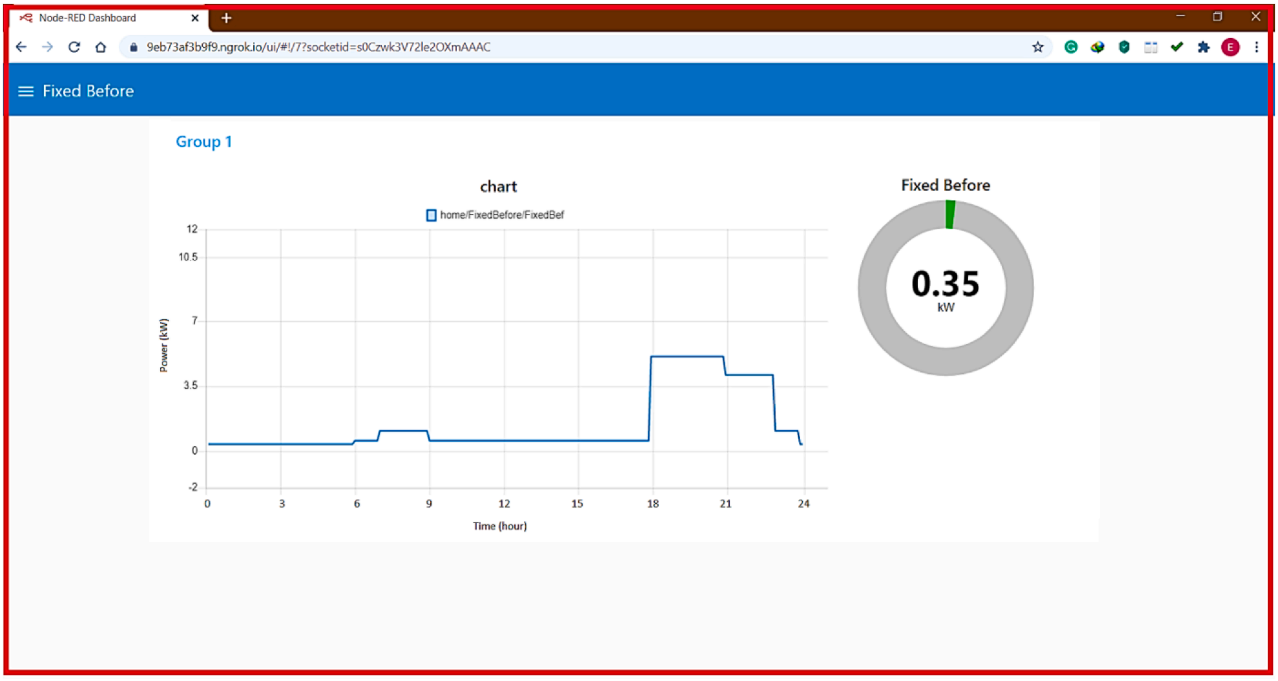

(a)

Fig. 18. Graphical user interface of daily microgrid demands performance with the proposed EMS. (a) fixed loads, (b) shift able loads, (c) non shift able loads.

without energy management system. The *CO*2 has been reduced with a peak demand decrease, as shown in Fig. 17.

Results discussion

The performance analysis of microgrid has been examined using electricity emission cost reduction, cost-saving, and PAR. After application of proposed energy management system, the time slots demanded for non-shift-able and shift-able demand have been moved to morning duration where energy price of utility is low, as displayed in Fig. 18. Therefore, the load profile has been corrected as shift-able and non-shift-able devices of the customer can function in the time slots with low price. Thus, the energy cost of consumption has been lessened, emission cost has been diminished, and PAR has been upgraded. As a result, Fig. 17 provides a comparison between the normal microgrid load profile shown in Fig. 12 and microgrid load demand given in Fig. 18. This comparison is done with respect to emission cost, energy cost, and PAR. It is noteworthy that with the proposed energy management system, the microgrid consumed energy cost has been decreased from 842.65 cent to 442 cent (that is, 47.54% of the cost of operation). By applying the proposed energy management system, the emission cost gets improved by 33.51% carbon dioxide emission has been lessened, and PAR is reduced by 61.49% in comparison to the microgrid operation without energy management system. Moreover, applying the energy management system, with an incentive in utility pricing, the PAR and peak demand have been decreased. This has led to a substantial reduction in the peak value of the load and, as a result, the power requirement from utility. Even though for the same load, the power consumed from the utility is not different in case of without energy management system, and with energy management system, the carbon dioxide has been reduced as there is a reduction in the peak demand, as shown in Fig. 17.

Fig. 19 displays the energy consumed from utility without and with proposed energy management system. It is demonstrated that energy consumption cost from the utility has been decreased by applying the proposed energy management system. Moreover, profile of energy have been enhanced over day time slots by motivating customers to move usage of their devices to low price utility timings. With an improvement in PAR, there is a reduction in the peak energy, as displayed in Fig. 19. Fig. 20 displays the battery performance where the process of battery discharging and charging depends on available output power of the PV system (as presupposed in this work). For the proposed energy management system, operational cost of microgrid is improved by 26.2% compared to the normal microgrid without the use of proposed energy management system technique. Nonetheless, there is an improvement in the emission cost and reduction in PAR by 49.1% and 38.4%, respectively, compared to the normal microgrid load profile without application of proposed energy management system Fig. 21.

Conclusions

In this study, an IoT based Demand Side Energy Management System (EMS) is developed. This EMS allows for control and monitoring of devices from a single platform providing users the awareness of their energy consumption. This system can supplement the demand response and prepaid energy programs by providing awareness to the people regarding their usage of energy. Using the IoT as well as the optimisation technique, a sophisticated control and optimal demand side management microgrid scheme is proposed in this research. The demand side management system is adopted to improve the emission cost, energy cost and PAR of the microgrid. In this research, we have presented the adoption of a cloud-based communication channel for appliances connected with the utility grid in the smart local areas. The use of the cloud computing platform provides the connectivity, data privacy, flexibility, interoperability, and the real-time features necessary for energy management. This research is a significant contribution to the literature related to smart home operation and it proposes Real-Time Electricity Scheduling (RTES) for HEM, which looks into the errors of information forecast. Unlike most of the previous HEM approaches that focus on

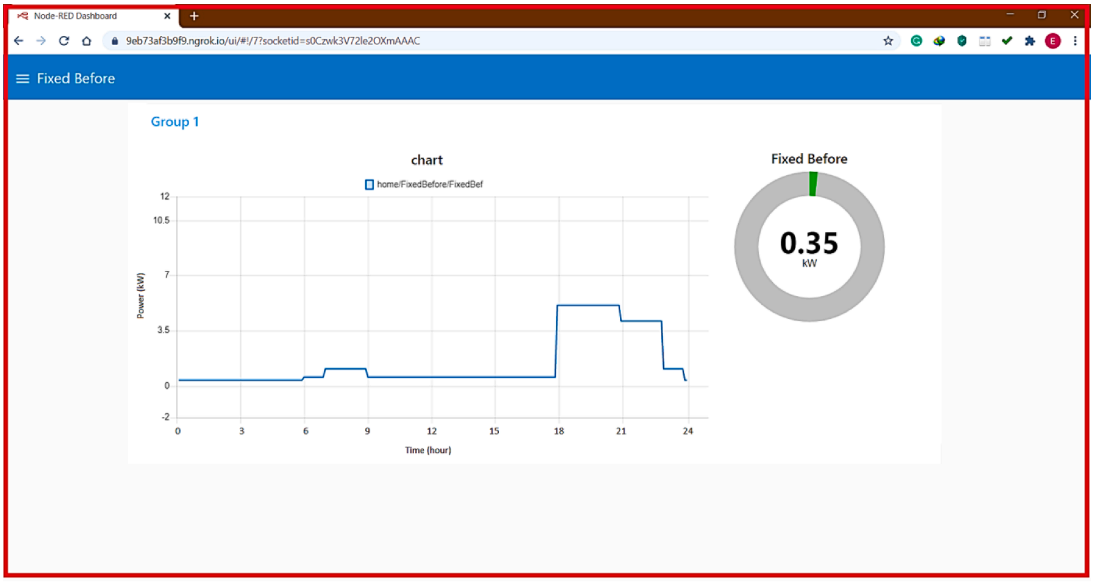

(a)

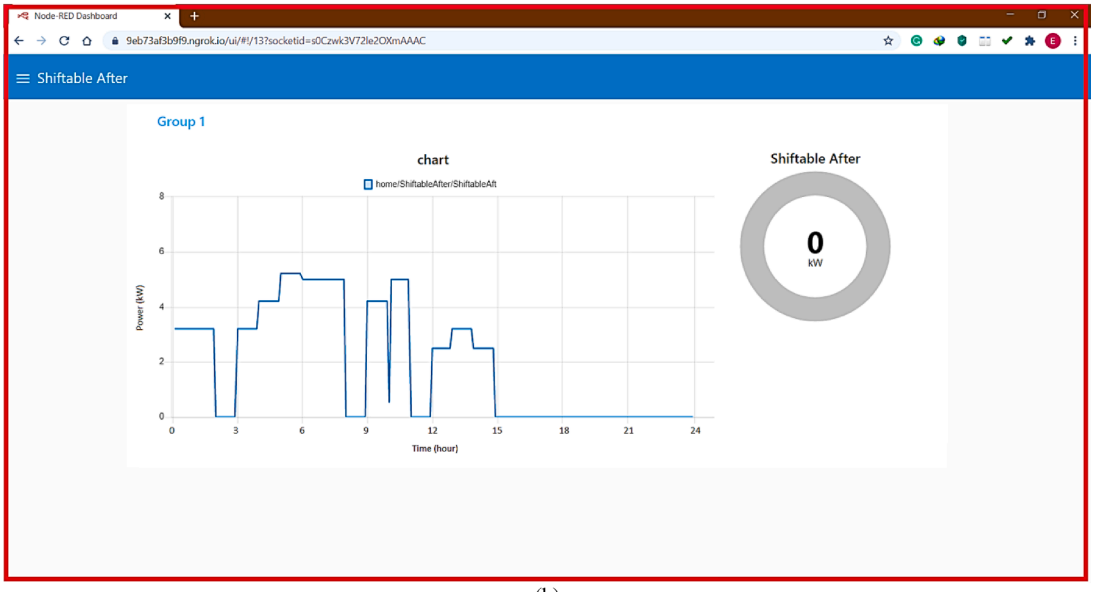

(b)

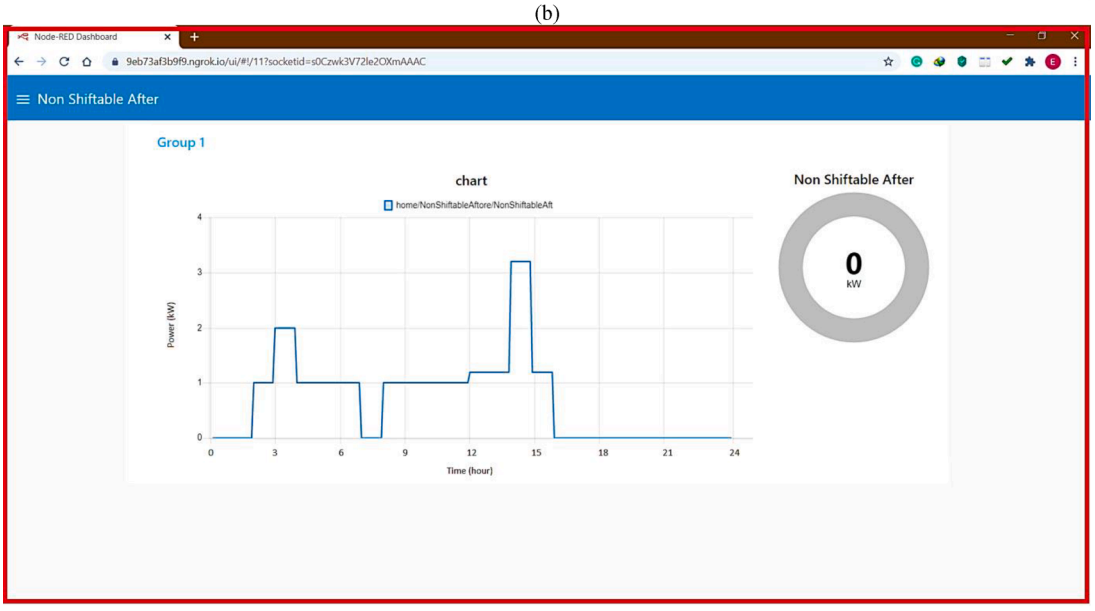

(c)

Fig. 18. (*continued*).

-

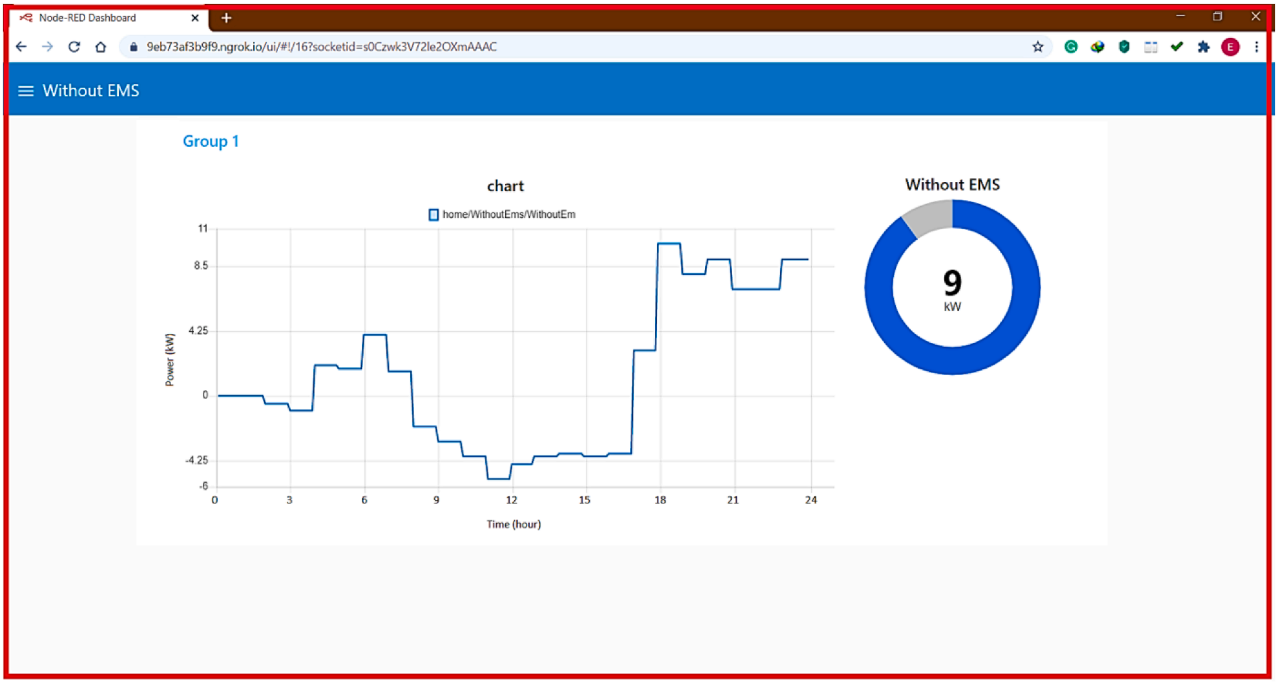

(a)

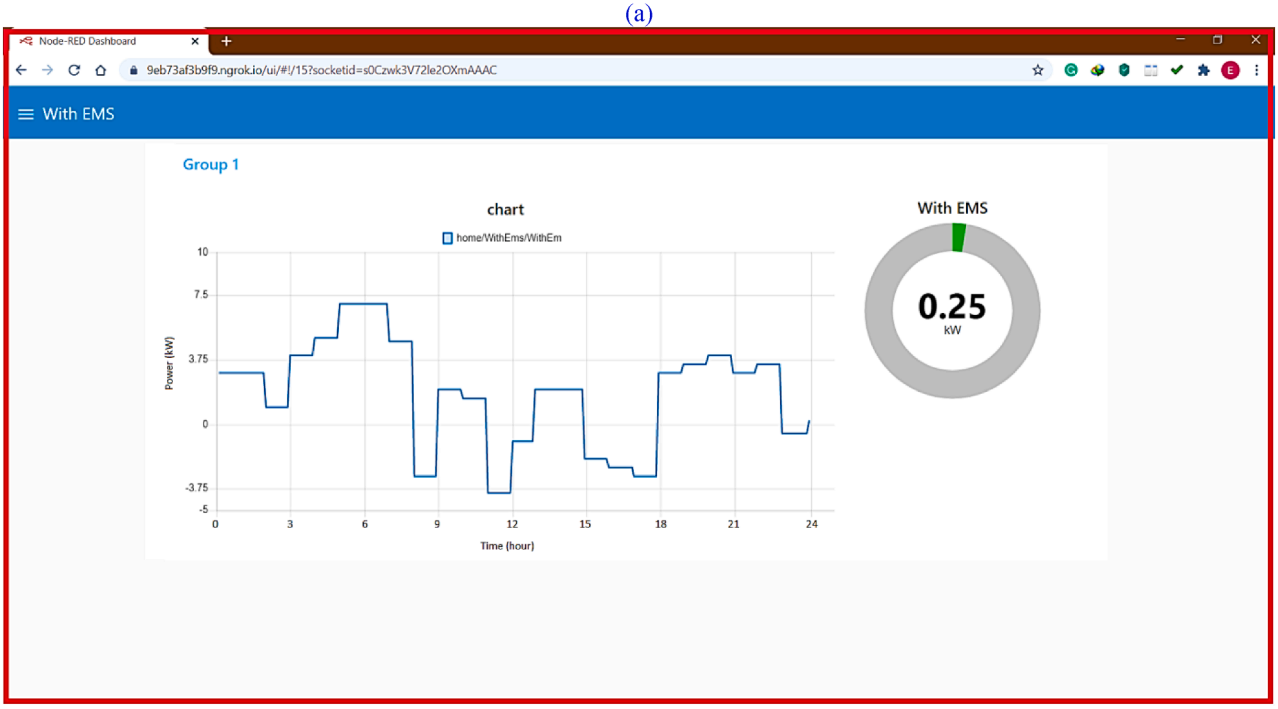

(b)

Fig. 19. Graphical user interface of daily utility power, (a) without proposed EMS, (b) with proposed EMS.

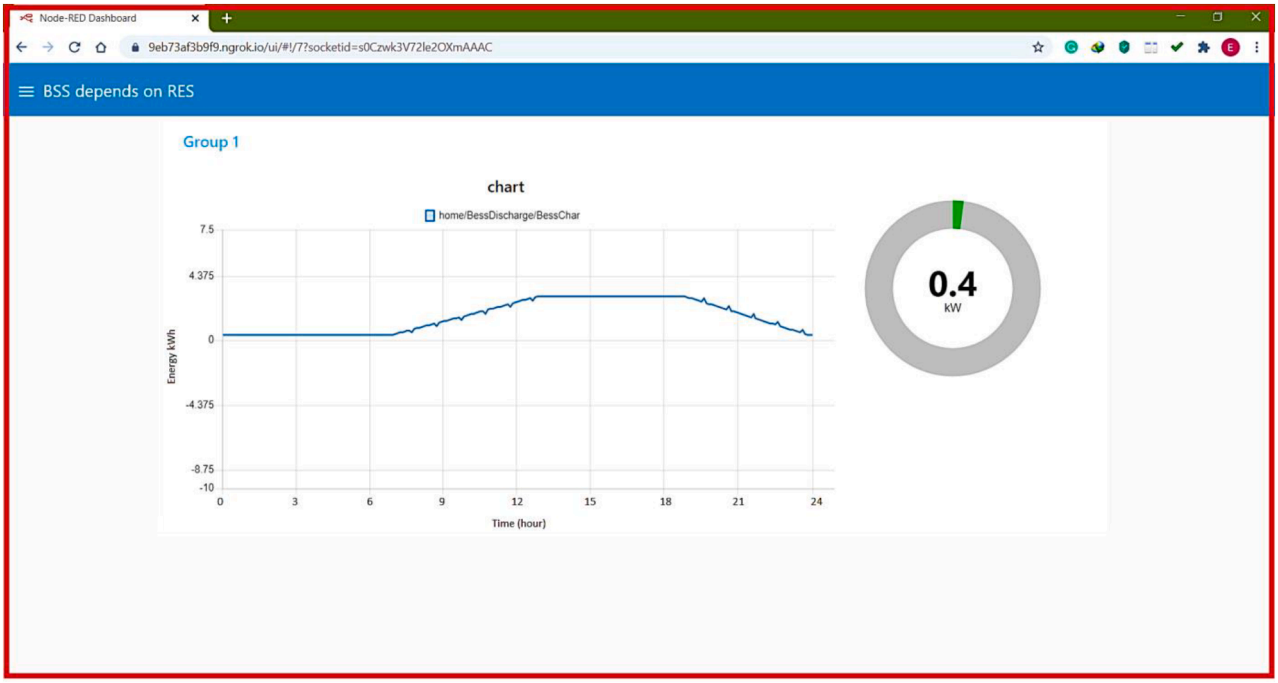

Fig. 20. Graphical user interface of daily energy storage performance based on renewable energy source output power.

Fig. 21. GUI of power factor after implement suggested power factor correction algorithm.

DAES (day-ahead electricity scheduling), we suggested a real-time scheduling system which ensures that the scheduling of every duration is the most sensible decision based on information forecast within the next 24 h. The proposed technique has a hierarchical structure with global and local communication layers which are based on HTTP TCP/IP and MQTT protocols for cloud interactions. The Wi-Fi is set up between the BSU controller and the TUs. It is also integrated with an innovative sophisticated self-diagnostic system so as to form a consistent network. Experimental outcomes demonstrate that the real-time system gives improved performance in comparison to DAES with respect to total electricity cost payment, and also HEM and RTES system integration can quickly take action when there is an unexpected change in the inputs. Using the suggested EMS scheme, the microgrid emission cost, energy cost, and PAR are decreased by 33.51%, 47.54%, and 61.49%, respectively, as compared to the microgrid without EMS for battery discharging and charging on the basis of the real utility price signal. For battery performances based on the output power of PV systems, the system performance is enhanced by 49.1%, 38.4%, 39.2% for emission

cost, energy cost, and PAR, respectively, as compared to the microgrid operation without EMS.

The newly devised closed-loop adaptive power factor controller presented in this paper is a highly effective device to offset the reactive power of quickly varying loads. This appliances have several features that make it highly promising for an extensive range of industrial applications. The innovative design ensures the most optimal compensation even when certain switching circuit components fail. To this point, the outcomes of the field test show that this device can provide nearly unity power factor at installation point regardless of dynamic changes in load reactive power. One more advantage of suggested device was that it could detect and control power factor correction remotely using the internet from anywhere in globe, enabling easy fine regulation of control parameters of technique to possibly achieve better functioning.

Declaration of Competing Interest

The authors declare that they have no known competing financial interests or personal relationships that could have appeared to influence the work reported in this paper.

References

[1] Yu Wang, Tung Lam Nguyen, Mazheruddin H. Syed, Yan Xu, Efren Guillo-Sansano, Van-Hoa Nguyen, Graeme Burt, Quoc-Tuan Tran, and Raphael Caire, " A Distributed Control Scheme of Microgrids in Energy Internet Paradigm and Its Multi-Site Implementation ", IEEE Transactions on Industrial Informatics, (Early Access), 2020, DOI: 10.1109/TII.2020.2976830.

[2] Hualei Zou; Yu Wang; Shiwen Mao; Fanghua Zhang; Xin Chen, "Distributed Online Energy Management in Interconnected Microgrids", IEEE Internet of Things Journal 7(4), 2020, 2738 – 2750. DOI: 10.1109/JIOT.2019.2957158.

[3] Alhasnawi BN, Jasim BH, Anvari-Moghaddam A, Blaabjerg F. A new robust control strategy for parallel operated inverters in green energy applications. Energies 2020; 13(13):3480. https://doi.org/10.3390/en13133480.

[4] Bishoy E. Sedhom, Magdi M. El-Saadawi, M.S. El Moursi, Mohamed.A. Hassan, Abdelfattah A. Eladl, " IoT-based optimal demand-side management and control scheme for smart microgrid", International Journal of Electrical Power and Energy Systems, 127, 2021, 106674.

[5] Chamandoust H, Derakhshan G, Hakimi SM, Bahramara S. Tri-objective scheduling of residential smart electrical distribution grids with optimal joint of responsive loads with renewable energy sources. J Storage Mater 2020;27:101112. https://doi.org/10.1016/j.est.2019.101112.

[6] Sulaima MF, Dahlan NY, Yasin ZM, Rosli MM, Omar Z, Hassan MY. A review of electricity pricing in peninsular Malaysia: Empirical investigation about the appropriateness of enhanced time of use (ETOU) Electricity Tariff. Renew Sustain Energy Rev 2019;110:348–67.

[7] Abdel-Basset M, Manogaran G, Mohamed M. Internet of Things (IoT) and its impact on supply chain: A Framework for Building Smart, Secure and Efficient Systems. Future Generation Comput Syst 2018;86:614–28.

[8] Bedi G, Venayagamoorthy GK, Singh R, Brooks R, Wang KC. Review of internet of things (IoT) in electric power and energy systems. IEEE Internet Things J 2019;5 (2):847–70. https://doi.org/10.1109/JIOT.2018.2802704.

[9] Al-Turjman F, Abujubbeh M. IoT-Enabled Smart Grid Via SM: An Overview. Future Generation Comput Syst 2019;96:579–90.

[10] Li S, Yang J, Song W, Chen An. A real-time electricity scheduling for residential home energy management. IEEE Internet Things J 2019;6(2):2602–11. https://doi.org/10.1109/JIoT.648890710.1109/JIOT.2018.2872463.

[11] Musleh AS, Yao G, Muyeen SM. Blockchain applications in smart grid-review and frameworks. IEEE Access 2019;7:86746–57.

[12] Golpîra H, Bahramara S. Internet-of-things-based optimal smart city energy management considering shiftable loads and energy storage. J Cleaner Prod 2020; 264:121620. https://doi.org/10.1016/j.jclepro.2020.121620.

[13] Alhasnawi BN, Jasim BHJ. A novel hierarchical energy management system based on optimization for multi-microgrid. Int J Electr Eng Inform 2020;12(3):586–606. https://doi.org/10.15676/ijeei10.15676/ijeei.2020.12.310.15676/ijeei.2020.12.3.10.

[14] Vardakas JS, Zorba N, Verikoukis CV. Power demand control scenarios for smart grid applications with finite number of appliances. Appl. Energy 2016;162:83–98. https://doi.org/10.1016/j.apenergy.2015.10.008.

[15] Li C, Yu X, Yu W, Chen G, Wang J. Efficient computation for sparse load shifting in demand side management. IEEE Trans Smart Grid 2017;8(1):250–61. https://doi.org/10.1109/TSG.2016.2521377.

[16] Vagdoda J, Makwana D, Adhikaree A, Faika T, Kim T. "A Cloud-Based Multiagent System Platform for Residential Microgrids Towards Smart Grid Community ", *IEEE Power & Energy Society General Meeting (PESGM)*, Portland December 2018;24. https://doi.org/10.1109/PESGM.2018.8586459.

[17] Wang Yu, Nguyen T-L, Xu Y, Tran Q-T, Caire R. Tung-Lam Nguyen; Yan Xu; Quoc-Tuan Tran; Raphael Caire, "Peer-to-Peer Control for Networked Microgrids: Multi-Layer and Multi-Agent Architecture Design ". IEEE Trans Smart Grid (Early Access) 2020;11(6):4688–99. https://doi.org/10.1109/TSG.516541110.1109/TSG.2020.3006883.

[18] Wang K, Li H, Maharjan S, Zhang Y, Guo S." Green energy scheduling for demand side Management in the Smart Grid", Wang K, Li H, Maharjan S, Zhang Y, Guo S. "Green energy scheduling for demand side Management in the Smart Grid", IEEE Transactions on Green Communications and Networking, Volume: 2, Issue: 2, June 2018.

[19] Yaghmaee Moghaddam MH, Leon-Garcia A. A fog-based internet of energy architecture for Transactive energy management systems. IEEE Int Things J 2018;5 (2):1055–69.

[20] Hashmi SA, Ali CF, Zafar S. Internet of things and cloud computing based energy management system for demand-side management in smart grid. Int J Energy Res 2021;45(1):1007–22. https://doi.org/10.1002/er.v45.110.1002/er.6141.

[21] IEEE Trans Green Commun Netw. 2018;2(2):596-611. Sima Davarzani, Ramon Granella, Gareth A. Taylor, Ioana Pisica, "Implementation of a novel multi-agent system for demand response management in low-voltage distribution networks", Applied Energy, 2019, 253 (1), 113-516, DOI: 10.1016/j.apenergy.2019.113516.

[22] Golmohamadi H, Keypour R, Bak-Jensen B, Pillai JR. A multi-agent based optimization of residential and industrial demand response aggregators. Int J Electr Power Energy Syst 2019;107:472–85. https://doi.org/10.1016/j.ijepes.2018.12.020.

[23] Cortés-Arcos T, Bernal-Agustín JL, Dufo-López R, Lujano-Rojas JM, Contreras J. Multi-objective demand response to real-time prices (RTP) using a task scheduling methodology". Energy 2017;138:19–31. https://doi.org/10.1016/j.energy.2017.07.056.

[24] Bilal Naji Alhasnawi, Basil H. Jasim, " Adaptive Energy Management System for Smart Hybrid Microgrids", The 3rd Scientific Conference of Electrical and Electronic Engineering Researches (SCEEER), 2020, (15-16) JUNE 2020 | BASRAH / IRAQ,. DOI: 10.37917/ijeee.sceeer.3rd.11.

[25] Al-Ali AR, Zualkernan IA, Rashid M, Gupta R, AliKarar M. A smart home energy management system using IoT and big data analytics approach. IEEE Trans Consum Electron 2017;63(4):426–34. https://doi.org/10.1109/TCE.2017.015014.

[26] Ahmed MS, Mohamed A, Khatib T, Shareef H, Homod RZ, Ali JA. Real time optimal schedule controller for home energy management system using new binary backtracking search algorithm. Elsevier Energy and Build 2017;138:215–27. https://doi.org/10.1016/j.enbuild.2016.12.052.

[27] Marzal S, Gonzalez-Medina R, Salas-Puente R, Garcera G, Figueres E. An embedded internet of energy communication platform for the future smart microgrids management. IEEE Internet Things J 2019;6(4):7241–52. https://doi.org/10.1109/JIoT.648890710.1109/JIOT.2019.2915389.

[28] Mahapatra C, Moharana AK, Leung VM. "Energy Management in Smart Cities Based on Internet of Things. Peak Demand Reduction and Energy Savings ", *Sensors* 2017;17(12):2812. https://doi.org/10.3390/s17122812.

[29] Al Faruque MA, Vatanparvar K. Energy Management-as-a-Service Over Fog Computing Platform. IEEE Internet Things J 2016;3(2):161–9. https://doi.org/10.1109/JIOT.2015.2471260.

[30] Li WX, Logenthiran T, Phan VT, Woo WL. Implemented IoT based self-learning home management system (SHMS) for Singapore. IEEE Internet Things J 2018;5 (3):2212–9. https://doi.org/10.1109/JIOT.2018.2828144.

[31] Ciprian Mihai Coman, Adriana Florescu, and Constantin Daniel Oancea, "Improving the Efficiency and Sustainability of Power Systems Using Distributed Power Factor Correction Methods ", Sustainability, 2020, 12(8), 3134; DOI: 10.3390/su12083134.

[32] H.Jasim B, Naji Alhasnawi B. "Automated Power Factor Correction for Smart Home". Iraqi J Electr Electr Eng 2018;14(1):30–40. https://doi.org/10.33762/eeej.2018.144339.

[33] Cano-Ortega A, Sánchez-Sutil F, Hernandez JC. Power factor compensation using teaching learning based optimization and monitoring system by cloud data logger. Sensors 2019;19:2172. https://doi.org/10.3390/s19092172.

[34] Alhasnawi BN, Jasim BH, Dolores Esteban M. A New Robust Energy Management and Control Strategy for a Hybrid Microgrid System Based on Green Energy 2020; 12:5724.

[35] Muhammad Afzal, Qi Huang, Waqas Amin, Khalid Umer, Asif Raza, And Muhammad Naeem, "Blockchain Enabled Distributed Demand Side Management in Community Energy System With Smart Homes", IEEE Access (Volume: 8), Page (s): 37428 - 37439, DOI: 10.1109/ACCESS.2020.2975233.

[36] Alhasnawi BN, Jasim BH, Esteban MD, Guerrero JM. A novel smart energy management as a service over a cloud computing platform for nanogrid appliances. Sustainability 2020;12(22):9686. https://doi.org/10.3390/su12229686.

[37] Khalid A, Javaid N, Mateen A, Ilahi M, Saba T, Rehman A. Enhanced time-of-use electricity price rate using game theory. Electronics 2019;8(1):48. https://doi.org/10.3390/electronics8010048.

[38] George K. Adam, "DALI LED driver control system for lighting operations based on raspberry Pi and Kernel Modules ". Electronics 2019;8(9):1021. https://doi.org/10.3390/electronics8091021.

[39] Liu X, Zhang T, Ning Hu, Peng Zhang Yu, Zhang. The method of Internet of Things access and network communication based on MQTT. Elsevier Computer Commun 2020;153(1):169–76. https://doi.org/10.1016/j.comcom.2020.01.044.

[40] Raj, Jennifer S., Bashar, Abul, Ramson, S. R. Jino, "Innovative Data Communication Technologies and Application ", Lecture Notes on Data Engineering and Communications Technologies, 2019, Book, Springer. DOI: 10.1007/978-3-030-38040-3.

[41] Pouya Jamborsalamati, Edstan Fernandez, Mojtaba Moghimi, M. Jahangir Hossain, Alireza Heidari, and Junwei Lu "MQTT-Based Resource Allocation of Smart Buildings for Grid Demand Reduction Considering Unreliable Communication Links", IEEE Systems Journal, 2019, 13(3) , 3304 - 3315. DOI: 10.1109/JSYST.2018.2875537.

[42] Pradhan S, Ghose D. Amit Kumar Singh, "Impact of Power Factor Correction Methods on Power Distribution Network—A Case Study", *Advances in Greener Energy Technologies*. Springer 2020. https://doi.org/10.1007/978-981-15-4246-6_30.

[43] Yasin Kabir ; Yusuf Mohammad Mohsin ; Mohammad Monirujjaman Khan, "Automated power factor correction and energy monitoring system ", IEEE 2017 Second International Conference on Electrical, Computer and Communication Technologies (ICECCT), 2017, Coimbatore, India , 22-24 Feb, DOI: 10.1109/ICECCT.2017.8117969.

[44] Ciprian Mihai Coman. Adriana Florescu, and Constantin Daniel Oancea, " Improving the Effciency and Sustainability of Power Systems Using Distributed Power Factor Correction Methods". Sustainability 2020;12(8):3134. https://doi.org/10.3390/su12083134.